nature portfolio

Peer Review File

Solvation chemistry tailored via dielectric constant engineering for stable low-temperature aqueous zinc batteries

Corresponding Author: Professor Guiyin Xu

This file contains all reviewer reports in order by version, followed by all author rebuttals in order by version.

Version 0:

Reviewer comments:

Reviewer #1

(Remarks to the Author)
In this manuscript, the authors propose a solvation structure regulation mechanism dominated by dielectric constant, aiming to achieve stable cycling performance of aqueous zinc metal batteries at low temperatures. The assembled Zn||PANI full cell demonstrates an encouraging 100% capacity retention after 10,000 cycles. Unfortunately, most of the conclusions presented are neither novel nor original. Various aspects of the proposed mechanism have already been revealed by other researchers using similar strategies (Li, Xinpeng, et al. "Modulation of water reactivity by ethyl acetate/water co-solvent for zinc-metal batteries." Chemical Engineering Journal 487 (2024): 150588. Chen, Yuqing, et al. "Breaking solvation dominance of ethylene carbonate via molecular charge engineering enables lower temperature battery." Nature Communications 14.1 (2023): 8326.). In addition, the manuscript contains multiple apparent errors and lacks several important datasets necessary to support the claims. Therefore, I don't recommend it to be published.
1. The authors discuss the economic potential of EA in electrolyte formulation. However, we note that EA exhibits serious incompatibility with commonly used low-cost zinc salts. As a compromise, the authors employed zinc perchlorate, which is relatively expensive and not widely used in practical applications. Given that the zinc salt often constitutes a major component of the electrolyte, I am concerned about the practical viability and cost-effectiveness of using EA in real-world aqueous Zn battery systems.
2. The authors have to cite relevant literatures to support your statement " It is widely accepted that the form of ion association in high dielectric constant electrolytes consists of solvent-separated ion pairs, whereas those with a low dielectric constant primarily feature contact ion pairs".
3. The authors claim that solvent-separated ion pairs and contact ion pairs impede ion transport, while electrolytes with medium dielectric constants form a balanced ion association structure to enhance ion mobility. However, authors simultaneously assert that EA addition disrupts the hydrogen-bond network to facilitate ion transport. Please provide experimental and theoretical evidence to substantiate these claims. In addition, what is the difference between enhanced anion-cation pairing and contact ion pair?
4. The manuscript insufficiently addresses how low-ε solvents balance ion pair formation versus dissociation. The rationale for selecting EA as a co-solvent lacks systematic analysis; comparative experiments with other low-ε solvents are required to validate EA’s uniqueness or the theory’s general applicability.
5. In the sentence “Electrostatic portion of the metallic lithium is zero for both sides, as it is electrically neutral,” the mention of metallic lithium appears to be inconsistent with the rest of the manuscript, which focuses on zinc-based systems. This seems to be an oversight or a typographical error. Please revise it accordingly to maintain accuracy and consistency in terminology throughout the manuscript.
6. There appears to be a clear error in Fig. 1d regarding the DN of water. According to Gutmann’s widely cited work (Gutmann, V. "Empirical parameters for donor and acceptor properties of solvents." Electrochimica Acta 21.9 (1976): 661-670.), the donor number of liquid water is approximately 33, not 18, which corresponds to the gas phase. Please revise the value accordingly to ensure consistency with established empirical data.
7. The authors screened the optimal electrolyte formulation based on ionic conductivity derived from EIS measurements. However, no corresponding chronoamperometry data and EIS fitting results are provided. According to previous studies (Yang, Jin-Lin, et al. "Designing single-ion conductive electrolytes for aqueous zinc batteries." Matter 7.6 (2024): 1928-1949.), the impedance of aqueous Zn-ion batteries can be unstable. Therefore, for ionic conductivity measurements at different temperatures, we recommend the use of a conductivity meter to obtain more reliable and reproducible results.

Moreover, based on the data presented, the ionic conductivity of the 20(H2O):1(EA) electrolyte is comparable to that of the 16:1 formulation across various temperatures. Therefore, selecting 16:1 as the optimal concentration requires further justification, such as by comparing Coulombic efficiency, symmetric cell lifespan, or other electrochemical performance metrics.
8. The authors provided WT-EXAFS data in Fig. 2c, effectively visualizing the EXAFS signals. However, for rigorous validation and clarity of EXAFS fitting results, the authors are requested to also provide the original Zn K-edge EXAFS oscillation data (in k-space) and the corresponding fitting curves in R-space. Specifically, please include plots clearly showing the experimental and fitted EXAFS data overlaid in both k-space and R-space, along with a detailed summary table of structural parameters (coordination number, bond length, etc.). This information is essential for ensuring transparency, reproducibility, and robust evaluation of the EXAFS analysis.
9. The description of the in situ FTIR difference spectra is quite confusing. First, it is unclear whether the spectra shown in Fig. 3c and Fig. S14b correspond to HDCE or MDCE, the manuscript does not clarify this, leaving the reader uncertain. Second, the definitions of A(tx), A(t0), and A(tz) are not provided in the main text, and to the best of my knowledge, these are not standard or widely recognized terms. In Fig. S14c and d, there is also a clear inconsistency between the y-axis label and the figure captions. The axis label reads “A(t) - A(t0)”, while the caption refers to “A(tz) - A(t0)”, which are not equivalent concepts based on the definitions implied in the manuscript. This inconsistency is confusing and should be corrected to ensure clarity. Moreover, according to the authors, A(tz) represents the first spectrum collected after applying current and should therefore be time-independent. However, the spectral changes shown in the figure appear to vary over time, which contradicts that definition. Additionally, the observed enhancement of W-H relative absorbance for MDCE under biased potential deviates from previous reports in the literature (Yu, Xiaoyu, et al. "Unlocking dynamic solvation chemistry and hydrogen evolution mechanism in aqueous zinc batteries." Journal of the American Chemical Society 146.25 (2024): 17103-17113.). The authors should provide a clear explanation for this discrepancy. Lastly, important experimental details are missing, such as the duration of the charge/discharge process, spectral acquisition resolution, and the number of scans. Providing this information is necessary for readers to fully understand and evaluate the experimental setup and results.
10. Why does MDCE exhibit a significantly higher nucleation overpotential difference at –40°C compared to –50°C in Figure 4d?

Reviewer #2

(Remarks to the Author)
Comments (major strengths):
The paper reports a dielectric constant modulation strategy to improve the cryogenic performance of aqueous Zn metal batteries. By introducing a low-ε co-solvent (ethyl acetate, EA) into a $Zn(ClO_4)_2$ electrolyte, the authors successfully disrupt the hydrogen-bonding network of water, regulate Zn^{2+} solvation structure, and enable stable Zn plating/stripping under extreme cold conditions (down to –50 °C).
The study is thorough, well-executed, and presented. The approach is novel, and the conclusions are convincingly supported by complementary experimental and simulation data. The electrochemical results are outstanding, especially the symmetric Zn||Zn cycling for over 4,000 h at –50 °C and 10,000 cycles in PANI||Zn full cells.
The manuscript is generally well-organized and experimentally comprehensive. However, the following concerns should be addressed before publication.

Concerns (weaknesses):
1. Mechanistic ambiguity in “altering dielectric response”
The statement “$Zn(ClO_4)_2{\cdot}6H_2O$ enhances the miscibility of EA and water by altering the solution’s overall dielectric response” (page 5, paragraph 1) lacks sufficient mechanistic explanation. While it is suggested that the salt improves solvent compatibility, the phrase “altering dielectric response” remains vague. It would be helpful to clarify how $Zn(ClO_4)_2{\cdot}6H_2O$ influences the dielectric environment — for instance, by coordinating with water to reduce its effective polarity, by screening unfavorable interactions between EA and H_2O, or by modifying hydrogen bonding networks. A brief discussion or reference to a specific interaction model (e.g., salt-mediated dipole alignment or suppression of phase separation) would strengthen this point and aid the reader's understanding.

2. Spectral interpretation lacks quantification or deconvolution
The FTIR and Raman shifts (e.g., C–O–C from 1046 to 1040 cm^{-1}, O–Cl–O from 1079 to 1073 cm^{-1}) are invoked as evidence of solvation changes, but the authors present only qualitative discussion. There is no spectral deconvolution or integration data (e.g., peak area ratios) to quantify solvation shell reorganization or binding strength. Especially for the ClO_4^- shift, which is subtle, a clearer attribution is needed—could the observed change be due to simple dilution, not coordination? A deeper spectroscopic analysis would strengthen the claims.

3. Unclear link between hydrogen-bond shifts and network strength
The authors state that FTIR/Raman results (e.g., shifts in O–H vibrations) “promote the conversion of weak and medium-strength hydrogen bond networks to strong hydrogen bond networks,” which contradicts the usual interpretation that the addition of organic co-solvents weakens water’s H-bond network. The use of “strong H-bond network” here needs clarification: does this imply localized but fewer, stronger H-bonds or just a spectral artifact? Otherwise, the interpretation appears inconsistent to disrupt water structure to improve low-temperature performance.

4. Interpretation of OCP and solvation energy lacks control validation
The potentiometric measurement of solvation energy (OCP between asymmetric electrolytes) is elegant, but its accuracy depends on minimizing liquid junction potential and assuming identical Zn activity at both electrodes. While Supplementary

Discussion 1 outlines these assumptions, no control (e.g., symmetric electrolyte test, or multiple Zn salts) is shown to validate the result.

5. Contradiction in SEI formation logic
The authors propose that stronger Zn^{2+}–ClO_4^- pairing (enabled by lower ε) leads to SEI formation via ClO_4^- reduction. However, in aqueous systems, ClO_4^- is generally inert under standard potentials. No electrochemical or chemical evidence (e.g., cyclic voltammetry, ion chromatography) is provided to confirm ClO_4^- reduction or its conversion to SEI-forming species. Without this, the link between ion pairing and SEI composition remains speculative.

6. Insufficient mechanistic explanation for SEI formation promoted by EA
While the manuscript convincingly demonstrates the formation of a robust SEI layer in the MDCE system through cryo-TEM, XPS, and TOF-SIMS analysis, the underlying mechanism by which EA promotes SEI formation remains insufficiently explained. Given the known challenges in forming SEI in aqueous systems due to competitive HER, it is unclear how EA reduction products contribute to SEI nucleation and growth. Additionally, the possible synergistic decomposition of EA and ClO_4^- is not well discussed.
Suggested revision: Please clarify the role of EA in SEI formation at the molecular level. Is there any evidence of EA-derived species (e.g., acetate) directly contributing to SEI structure? Including reaction pathway analysis or DFT simulations would significantly strengthen the mechanistic claims.

7. ClO_4^- decomposition pathway and its role in Zn corrosion is under-supported
The authors attribute Zn corrosion in the HDCE system to Cl^- derived from ClO_4^- decomposition. However, ClO_4^- is generally considered electrochemically inert under standard aqueous conditions, and the manuscript lacks direct evidence for its decomposition. This assertion is critical, as it underpins the comparison between HDCE and MDCE degradation behavior.
Suggested revision: Please provide additional evidence (experimental or theoretical) supporting ClO_4^- decomposition in HDCE. If referencing prior literature, a discussion of the relevant decomposition potential or conditions under which ClO_4^- becomes reactive would improve clarity and credibility.

Reviewer #3

(Remarks to the Author)
In this work, the author proposed a strategy for low-temperature ZMBs based on tailoring the Zn2+ solvation environment by engineering the dielectric constant. Specifically, according to introduction of EA into Zn(ClO4)2 electrolyte to weaken water's hydrogen-bond network and increase cation-anion pairing. This strategy accelerates $Zn2^+$ transport and desolvation, promotes the formation of a protective solid electrolyte interphase rich in organic and inorganic components, and inhibits parasitic hydrogen evolution. Although it achieves excellent electrochemical performance for the cryogenic aqueous zinc batteries, many issues should be addressed before publication.

1. It is mentioned that Zn(ClO4)2·6H2O enhances the miscibility of EA and water by altering the solution's overall dielectric response. In the method section, the calculation method and equation of dielectric constants of hybrid salt and solvent (such as Zn(ClO4)2/EA, Zn(ClO4)2 EA/H2O) are not clear. Please supplemented the section.
2. The author proposed that EA is an ideal co-solvent because it has a low dielectric constant, low viscosity, and low freezing point. But as can be seen from Table S1, MeOH and THF also have similar characteristics. Besides, other carboxylic esters, such as methyl acetate and methyl formate also have similar characteristics. Why EA was chosen as the co-solvent, the explanation is not sufficient.
3. The results of Figure S1 show that ZnOTF also enables EA to form a homogeneous solution with H2O, so why not choose ZnOTF instead of ZnClO4?
4.. In Line 165, it is stated that weak and medium hydrogen bonding networks evolve to strong hydrogen bonding networks, but the statement is contrary to the cited reference.
5. The results of Fig. 3a, b seem to contradict each other with Fig. 3a showing that MDCE has a greater solvation energy, while the opposite is true for Fig. 3b.
6. Figure S13 only shows that it is easier to remove water molecules in the solvated configuration containing EA formed in the electrolyte after the addition of EA, while the ability of EA to replace some of the water molecules suggests that it has a stronger bonding force with Zn2+, which may cause a greater obstruction in the removal of EA molecules and ions. Is the statement in the abstract that the modified solvated structure accelerates Zn2+ desolvation not appropriate?

Reviewer #4

(Remarks to the Author)
The work by Zhu and co-workers presented the performance and characterization of ZnClO4 aqueous electrolytes with or without EA additive. The electrolyte with EA, MDCE, showed superior performance compared to the aqueous counterpart, HDCE, especially at low temperature. The study combined various experimental and simulation techniques and insightful details were provided for the studied systems.

1) The work emphasized “dielectric engineering” in the title. However, the meaning of which is not very clear to me. The study included two electrolytes, one with relative high dielectric and the other one lower. Is the dielectric the decisive reason for the superior performance? If one uses a different additive to prepare an electrolyte with the same dielectric, or even a completely different electrolyte with the same dielectric constant, would the same performance be expected? Or is the performance reported in the work specific for EA at the studied composition?

2) Other specific comments:
a) Line 130, “pure electrolyte” likely means “pure aqueous electrolyte”, but it could also mean “pure EA electrolyte”. Please clarify.
b) Line 138: “nEA:nH2O” should be “EA:H2O”.
c) Starting from Line 155, the authors discussed the FTIR results. The authors mentioned “red shift” and “blue shift”, but it is hard to see from the context the shifts are relative to what. On lines 162-163, the terms “left shift” and “right shift” were used whereas Figures 2a and 2b show FTIR in opposite frequency orders, which make it hard to follow. These terms are not professional either. Opposite x-axis is also seen in Figure 6 in SI. Please make it consistent throughout the paper.
d) Line 185 mentioned average number of HB but it is not clear average over what? Are the numbers per water molecule or per acceptor site or any other definition?
e) For the FTIR results shown in Figure 2, what is the temperature? Does FTIR show the same temperature dependent trend as the simulation? Temperature is not provided for most of the results reported in the manuscript.
f) The sentences on lines 229-233 are hard to follow. In the beginning it mentioned “immobilization of the ClO4- anion”, what does “immobilization” mean here? Then it talks about solvents: “solvents with stronger binding properties tend to produce more negative solvation energies”. In the next sentence, it goes back to ion: “corresponding to a greater number of ion pairs.” Then the final part, what does “reduced ion dissociation” mean? Is this about structure or kinetics?
g) Lines 240-241: E_a were reported for HDCE and MDCE, and commented that “the latter (MDCE) being notably lower than …” The E_a of HDCE and MDCE are only 1.2 kJ/mol different from each other, which is lower than kT. These E_a are similar to me.
h) Line 578 says the OPLS-AA force field was used in the study. Does OPLS-AA include parameters for Zn2+ ion? If not, please specify what model was used for Zn2+.
i) For the simulation study, validation of the force field needs to be provided.

Overall, the work presented a systematic study of an electrolyte system and insightful results were reported. An emphasis on dielectric engineering was made. However, it is not clear what the authors mean by “dielectric engineering”. On the other hand, the effect of dielectric constant has been discussed in the literature. Works on low temperature electrolyte are available in the literature too. Therefore, I do not think the work carry enough novelty to be published in Nature Communication. I would suggest the authors address above comments and resubmit it to a different journal.

Version 1:

Reviewer comments:

Reviewer #1

(Remarks to the Author)
This manuscript has been revised as the comments, so it is suitable for publication without change.

Reviewer #2

(Remarks to the Author)
The authors provided a complete response to my questions. I suggest the consideration of this work.

Reviewer #3

(Remarks to the Author)
All my questions have been well addressed. It can be accepted in this journal.

Reviewer #4

(Remarks to the Author)
The authors addressed most of my comments. But critical details of the MD simulations are still missing. The authors said an optimized Zn2+ model was used in the study. The parameters, reference and/or other optimization details should be provided so that readers can reproduce the work.

Proper validation of the used force fields parameters for the studied systems are also needed. General force fields like OPLS can work on one system but fail badly on another. The choice of water model and other simulation protocols can change the results too. In spite of the references provided, direct comparison with experimental measurement on the same systems should be provided.

Version 2:

Reviewer comments:

Reviewer #4

(Remarks to the Author)
The authors provided more simulation details including information about the force field parameters in the revised manuscript. Considering the fact that simulation is only part of this work, I would support the publication of the work if the authors can provide input files for the simulation in the SI, including enough information about simulation details and all the force field parameters that others can reproduce the work.
Meanwhile, I want to make it clear to the authors that consistent results using two sets of force fields do not necessarily validate the simulation results. As I commented previously, a direct comparison with experimental measurements on the same system under the same condition is needed for this purpose.

Point-by-point response to the reviewers' comments

We thank the reviewers for their careful assessment. Their comments led us to substantially strengthen the manuscript: we clarified the scope and novelty of our dielectric-engineering strategy, added mechanistic evidence and controls, corrected inaccuracies, and refined the presentation. The revised manuscript and the point-by-point response address every comment with new analyses, data, and citations. All textual changes are highlighted in yellow.

Click to go to responses to a specific reviewer:

Reviewer #1 Reviewer #2 Reviewer #3 Reviewer #4

RESPONSE TO REVIEWERS' COMMENTS

Reviewer #1:

In this manuscript, the authors propose a solvation structure regulation mechanism dominated by dielectric constant, aiming to achieve stable cycling performance of aqueous zinc metal batteries at low temperatures. The assembled Zn||PANI full cell demonstrates an encouraging 100% capacity retention after 10,000 cycles. Unfortunately, most of the conclusions presented are neither novel nor original. Various aspects of the proposed mechanism have already been revealed by other researchers using similar strategies (Li, Xinpeng, et al. "Modulation of water reactivity by ethyl acetate/water co-solvent for zinc-metal batteries." Chemical Engineering Journal 487 (2024): 150588. Chen, Yuqing, et al. "Breaking solvation dominance of ethylene carbonate via molecular charge engineering enables lower temperature battery." Nature Communications 14.1 (2023): 8326.). In addition, the manuscript contains multiple apparent errors and lacks several important datasets necessary to support the claims. Therefore, I don't recommend it to be published.

Response: We greatly appreciate the reviewer's valuable comments. As mentioned by the reviewer, EA and similar ester solvents have been reported for zinc/lithium metal batteries. However, this study presents differences in mechanisms compared to previous research. In the article "Breaking solvation dominance of ethylene carbonate via molecular charge engineering enables lower temperature battery." Nature Communications 14, 1 (2023): 8326. Chen et al. aim to facilitate the coordination of low-ε solvents with Li^+ to occupy its coordination sites, thereby converting solvent-separated ion pairs (SSIPs) from high-ε solvent-dominated to low-ε-dominated. This work targets zinc batteries with aqueous electrolytes, where the strong hydrogen-bond network of water at low temperatures sharply reduces ionic conductivity. We propose a dielectric matching strategy to construct an electrolyte with a moderate dielectric constant ($\varepsilon \approx 25.25$), enabling synergistic regulation of Zn^{2+} solvation and accelerating Zn^{2+} transport and desolvation. Compared with CEJ (Li, Xinpeng, et al., Chemical Engineering Journal 487 (2024): 150588.), this work employs a different electrolyte composition (EA/H_2O = 1:16 vs. 1:6), achieves higher ionic conductivity and better performance at lower temperatures (−50 °C vs. −40 °C), and uses a different zinc salt ($Zn(ClO_4)_2$ vs. $Zn(CF_3SO_3)_2$) for bilayer SEI. Li et al. and other researchers have

mainly focused on how co-solvents regulate solvation structures to improve low-temperature performance. Still, they lack an in-depth investigation into how interfacial solvation structures evolve under an electric field and their role in promoting SEI formation.

Instead, our contribution is to (i) define and target a medium-ε window (ε≈25) that balances dissociation and ion pairing and (ii) quantify interfacial solvation dynamics under applied current that link this window to fast, stable Zn plating at low temperature. The revised text now presents dielectric engineering as a practical screening criterion, including permittivity range and solvation/interfacial checks. We have supplemented and corrected the data omissions and errors in the full text. We hope these clarifications and additions address the reviewer's concerns about novelty.

Our work presents three fundamental advancements that distinguish it from the existing literature:

1) Design strategy.

We proposed a dielectric matching strategy, wherein high-ε solvents promote the dissociation of zinc salts. In contrast, low-ε solvents optimize interface stability and ion transport kinetics at low temperatures. In this work, we selected H_2O/EA (molar ratio 16:1) to construct an electrolyte system with a moderate dielectric constant (ε≈25.25). This design has the following advantages: 1: Greater flexibility in composition: the dielectric environment of the electrolyte can be precisely controlled by adjusting the ratio of high/low dielectric constant solvents. 2: practical screening criterion: providing a quantifiable preliminary screening criterion for the design of low-temperature-resistant aqueous electrolytes.

2) Interfacial mechanism under bias (novelty).

The combination of in-situ infrared/confocal microscopy and theoretical calculations elucidates interfacial dynamics and decomposition mechanisms under an electric field. It further demonstrates that incorporating organic solvents with low dielectric constants facilitates the formation of a bilayer SEI, providing insights into solid-liquid interfaces and solvation dynamics that are crucial for cryogenic aqueous batteries.

3) Advanced electrochemical performance.

The MDCE Zn||Zn cell cycled for 4,000 h at −50 °C and >10 months at 25 °C, and a negligible capacity decay in low-temperature full cells over 12000 cycles, exceeding those of reported low-temperature aqueous ZMBs (Supplementary Fig. 22).

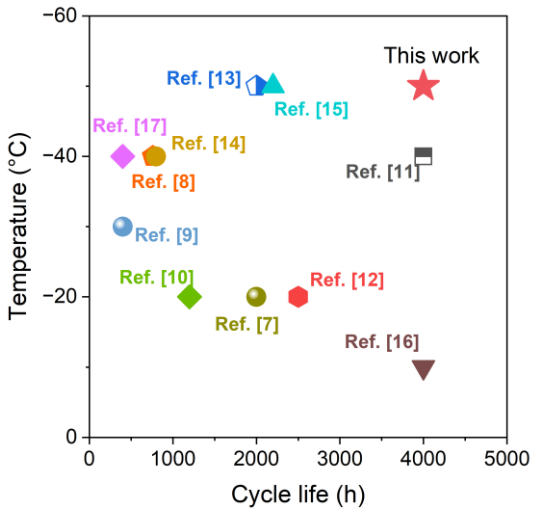

Supplementary Fig. 22 Comparison of the cycle life values of aqueous electrolyte in Zn||Zn cells at −50 °C-0 °C[7-17].

Comment 1. The authors discuss the economic potential of EA in electrolyte formulation. However, we note that EA exhibits serious incompatibility with commonly used low-cost zinc salts. As a compromise, the authors employed zinc perchlorate, which is relatively expensive and not widely used in practical applications. Given that the zinc salt often constitutes a major component of the electrolyte, I am concerned about the practical viability and cost-effectiveness of using EA in real-world aqueous Zn battery systems.

Response: Thank you for the suggestions. We will clarify this from the following two aspects:

1. **Compatibility and generality.** We agree that solvent–salt compatibility is a constraint. We therefore screened multiple zinc salts in EA:H_2O and report that both $Zn(ClO_4)_2$ and $Zn(CF_3SO_3)_2$ form single-phase electrolytes at EA:H_2O=1:16 (molar). $Zn(ClO_4)_2$ was selected because it provides higher low-temperature conductivity and better interfacial kinetics at the same composition; the $Zn(CF_3SO_3)_2$ control is now included to demonstrate that our approach is not

specific to ClO_4^- (conductivity at −50 °C: 24.92 vs 10.56 mS cm^{-1} at 1:16; corresponding CE and nucleation metrics are provided).

2. **Electrolyte economy**. This inventory of other salts, such as $ZnCl_2$, requires high concentrations (7-30 mol L^{-1}) to achieve similar performance (*Nat. Sustain.* 6, 325–335 (2023), *Nat. Commun.* 11, (2020) 4463), while relying on co-solvents like ethylene glycol (EG) may significantly reduce ion transport efficiency due to a sharp increase in viscosity at low temperatures (*Nat. Sustain.* 5, 205–213 (2022)). According to Table S3, i.e. 0.296 USD/g × 7 mol/L × 136 g/mol = 281 USD/L for $ZnCl_2$ electrolyte and 0.336 USD/g × 2 mol/L × 372.38 g/mol = 250 USD/L for $Zn(ClO_4)_2$ electrolyte. $Zn(ClO_4)_2.6H_2O$ shows lower cost. Furthermore, $Zn(ClO_4)_2$ demonstrates superior solubility, allowing high cycling stability and rapid reaction kinetics to be achieved under low-temperature conditions.

Compared to other aqueous electrolytes and ester-based organic electrolytes, the electrolyte system proposed in this study shows significant advantages in cost-effectiveness and adaptability to extreme environments. In subsequent research, we will systematically investigate the incompatibility mechanisms of other low-cost zinc salts in the EA/H_2O system and pursue effective regulation strategies to achieve electrolyte systems that combine cost advantages with high performance.

Comment 2. The authors have to cite relevant literatures to support your statement " It is widely accepted that the form of ion association in high dielectric constant electrolytes consists of solvent-separated ion pairs, whereas those with a low dielectric constant primarily feature contact ion pairs".

Response: Thank you for the suggestions. According to the reviewer's recommendation, we adjusted the literature references after the statement in the manuscript on page 5, line 126:

"It is widely accepted that the form of ion association in high dielectric constant electrolytes consists of solvent-separated ion pairs, whereas those with a low dielectric constant primarily feature contact ion pairs[21,30], both scenarios are detrimental to ion transport."

[21] Yao, N. et al. An atomic insight into the chemical origin and variation of the dielectric constant in liquid electrolytes. *Angew. Chem., Int. Ed.* 60, 21473-21478 (2021).

[30] Marcus, Y. & Hefter, G. Ion Pairing. *Chem. Rev.* 106, 4585-4621 (2006).

The corresponding description in the references is as follows: "A high dielectric constant is beneficial for the dissociation of cations and anions of salts and achieving high ionic conductivity". (*Angew. Chem., Int. Ed.* 60, 21473-21478 (2021) "…For solvents with high relative permittivity and electrolytes with low charges, the cutoff distance q is smaller than a. Therefore, no ion pairing takes place in such cases, such as, e.g., for the larger alkali halides in water, where q = 0.357 nm at 298.15 K. Smaller ions and ions with higher charges, especially in solvents with lower permittivity, should associate to ion pairs to extents given by eqs 2 and 9…" *Chem. Rev.* 106, 4585-4621 (2006).

Comment 3. The authors claim that solvent-separated ion pairs and contact ion pairs impede ion transport, while electrolytes with medium dielectric constants form a balanced ion association structure to enhance ion mobility. However, authors simultaneously assert that EA addition disrupts the hydrogen-bond network to facilitate ion transport. Please provide experimental and theoretical evidence to substantiate these claims. In addition, what is the difference between enhanced anion-cation pairing and contact ion pair?

Response: Thank you for the comment. At room temperature, solvent-separated ion pairs (SSIP) determine the number of charge carriers available for transport in electrolytes. High-dielectric-constant solvents, such as water, effectively dissociate ion pairs, creating abundant charge carriers and enabling efficient ion transport. HDCE contains more SSIP structures, resulting in higher ionic conductivity at room temperature (Fig. R1a). However, at ultra-low temperatures (−50 °C), ionic conductivity drops dramatically due to strengthened hydrogen bonding and the freezing of water, which disrupts ion mobility.

Conversely, low-dielectric-constant solvents can significantly mitigate freezing issues but suffer from limited ion dissociation, resulting in fewer charge carriers and reduced conductivity. Our method addresses both problems simultaneously: incorporating ethyl acetate (EA) into water

disrupts hydrogen bonding among water molecules and prevents ice formation, while preserving water's excellent solvating properties. This maintains a high concentration of charge carriers and enables efficient ion movement even at ultra-low temperatures (−50 °C)

The introduction of EA significantly lowers the freezing point of the electrolyte, thereby improving low-temperature performance. Meanwhile, the presence of contact ion pairs (CIP) can promote the formation of a stable solid electrolyte interface (SEI). However, as the EA content further increases, the concentration of CIP also rises (as shown by Raman spectroscopy and MD simulations), which hinders ion migration and consequently reduces the ionic conductivity of the electrolytes (Fig. R1a and Supplementary Table 4). This trend is clearly observable in conductivity tests. The key point is to regulate the concentration of CIP to synergistically optimize the freezing point and ionic conductivity, thereby achieving optimal low-temperature electrochemical performance.

Additionally, the introduction of EA disrupts the hydrogen-bond network, thereby promoting improved ion transport. Molecular dynamics (MD) simulations were conducted to analyze the mean squared displacement (MSD) of zinc ions under both room temperature and low-temperature (−50°C) conditions. The results show that in MDCE ($Zn(ClO_4)_2$ H_2O/EA, molar ratios of EA: H_2O = 1:16), zinc ion mobility is lower than in HDCE ($Zn(ClO_4)_2$ H_2O) at room temperature, whereas at −50°C, MDCE demonstrates better zinc ion migration rates compared to HDCE (Fig. R1b, c).

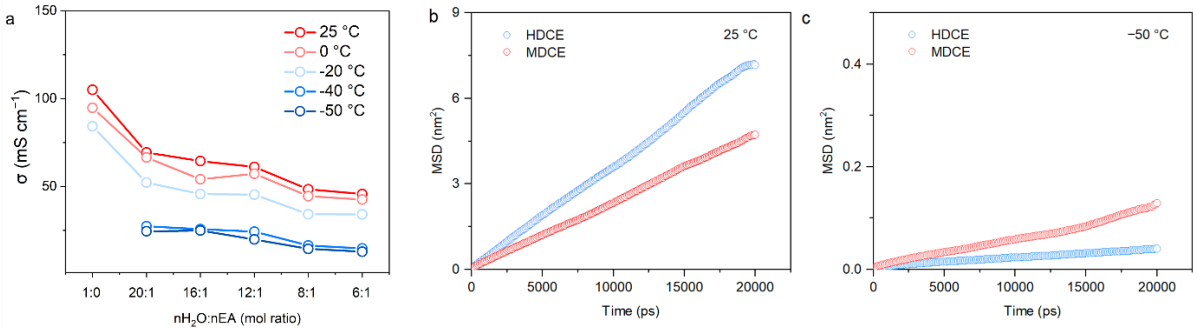

Fig. R1 a, Ionic conductivities of $Zn(ClO_4)_2$ H_2O/EA solutions with different H_2O/EA molar ratios from 1:0 to 6:1 at various temperatures, were obtained through measurements conductivity meter. b, c The MSD of the Zn^{2+} ion was calculated for both HDCE and MDCE at 25 °C (b) and −50 °C (c).

Lastly, the concepts of contact ion pairs and enhanced anion-cation pairs are not the same. The expression of "enhanced anion-cation pairs" is intended to indicate that the introduction of EA enhances the cation–anion combination. We have revised this ambiguous expression in the manuscript on page 4, line 107:

"…low dielectric constant solvents enhance cation-anion pairing…"

Comment 4. The manuscript insufficiently addresses how low-ε solvents balance ion pair formation versus dissociation. The rationale for selecting EA as a co-solvent lacks systematic analysis; comparative experiments with other low-ε solvents are required to validate EA's uniqueness or the theory's general applicability.

Response: Thank you for the suggestions. In our work, the high ε solvent is responsible for promoting ion pair dissociation in the electrolyte. Based on this, we formulated electrolytes with varying contents of low dielectric constant solvents to explore an optimal ratio that ensures sufficient ion dissociation while promoting moderate cation–anion association to support SEI formation at low temperature while retaining adequate ionic transport, resulting in improved battery performance.

In accordance with the reviewer's suggestions, we conducted experiments utilizing low dielectric constant co-solvents, specifically diethyl carbonate (DEC) (ε = 2.8), tetrahydrofuran (THF) (ε = 7.4), and methyl formate (MF) (ε = 8.5). Our findings reveal that the electrolyte with DEC led to macroscopic phase separation (Fig. R2). Notably, THF and MF did not exhibit any layering. Zn||Cu batteries were assembled to investigate zinc ion plating and stripping at both room and low temperatures. The electrolyte containing DEC resulted in an average Coulombic efficiency of 91.2% at room temperature and 96.66% at low temperature (−50 °C), which is markedly lower than that of other electrolytes. Furthermore, the nucleation overpotential at low temperature (η = 670 mV) was significantly higher than that observed with different electrolytes (Fig. R3).

These results suggest that electrolytes with moderate dielectric constants (for example, $Zn(ClO_4)_2$ EA/H_2O molar ratio EA: H_2O = 1:16, ε = 25.25) universally regulate solvation structures. Despite

having similar dielectric constants, THF and MF demonstrated poor electrochemical stability at room temperature. While MF and THF can serve as additives in organic low-temperature electrolytes, MF undergoes hydrolysis in aqueous electrolytes. EA exhibits superior stability compared to MF for the following reasons: (1) the carbonyl carbon in MF is more positively charged due to the weaker electron-donating ability of -H compared to -CH_3, rendering it more susceptible to nucleophilic attack. (2) In EA, the methyl group disperses the positive charge of the carbonyl carbon through hyperconjugation, thereby enhancing its stability. (March, J. (1992). Advanced Organic Chemistry (4th ed.). Wiley.). Similarly, THF belongs to the class of ether solvents. The oxygen in the ether group contains two lone pairs of electrons, which gives it basicity and nucleophilicity. Influenced by electronic effects, when there is a hydrogen on the α-carbon of the ether, it is prone to oxidation. (John M. Fundamentals of organic chemistry, 5th ed.), which can form peroxides or decompose under anodic conditions, leading to side reactions that degrade electrolyte performance and form unwanted byproducts. In contrast, EA, which belongs to carbonates, has better antioxidant properties.

Based on the research results mentioned above, we found that the introduction of co-solvents with low dielectric constants can effectively enhance the low-temperature performance of batteries. This phenomenon fully validates the universality of the electrolyte strategy with moderate dielectric constants. Notably, EA exhibits particularly outstanding low-temperature electrochemical performance due to its unique physicochemical properties, such as lower viscosity and suitable solvation ability. This provides an important design concept and research direction for the subsequent development of high-performance low-temperature resistant electrolyte systems.

We have added the corresponding content to the main text (page 8, line 225):

"Combining the results of ionic conductivity at various temperatures, incorporating low dielectric constant solvents (EA) facilitates ion transport at low temperatures, while maintaining a balance between sufficient ion pair dissociation and moderate cation-anion association. This facilitates stable SEI formation, ultimately enhancing battery performance."

We have also added the test results for other solvents to the supplementary information

(Supplementary Fig. 2 and Supplementary Note 2)：

"To systematically evaluate the impact of low dielectric constant co-solvents on the low-temperature performance of batteries, we selected a series of solvents with similar dielectric constants, specifically diethyl carbonate (DEC) (ε = 2.8), tetrahydrofuran (THF) (ε = 7.4), and methyl formate (MF) (ε = 8.5). Our findings reveal that the electrolyte with DEC led to macroscopic phase separation (Supplementary Fig. 2a). Notably, THF and MF did not exhibit any layering. Zn||Cu batteries were assembled to investigate zinc ion plating and stripping at both room and low temperatures. The electrolyte containing DEC resulted in an average Coulombic efficiency of 91.2% at room temperature and 96.66% at low temperature (−50 °C), which is markedly lower than that of other electrolytes. Furthermore, the nucleation overpotential at low temperature (η = 670 mV) was significantly higher than that observed with different electrolytes (Supplementary Fig. 2b, c). As a result, EA exhibits particularly outstanding low-temperature electrochemical performance. This provides an important design concept and research direction for the subsequent development of high-performance low-temperature resistant electrolyte systems."

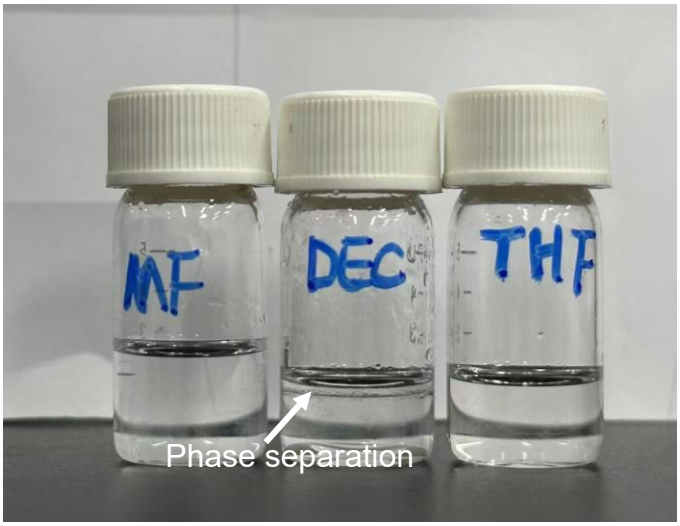

Fig. R2/Supplementary Fig. 2 Digital photograph of an electrolyte containing low dielectric constant solvents such as THF, DEC, and MF.

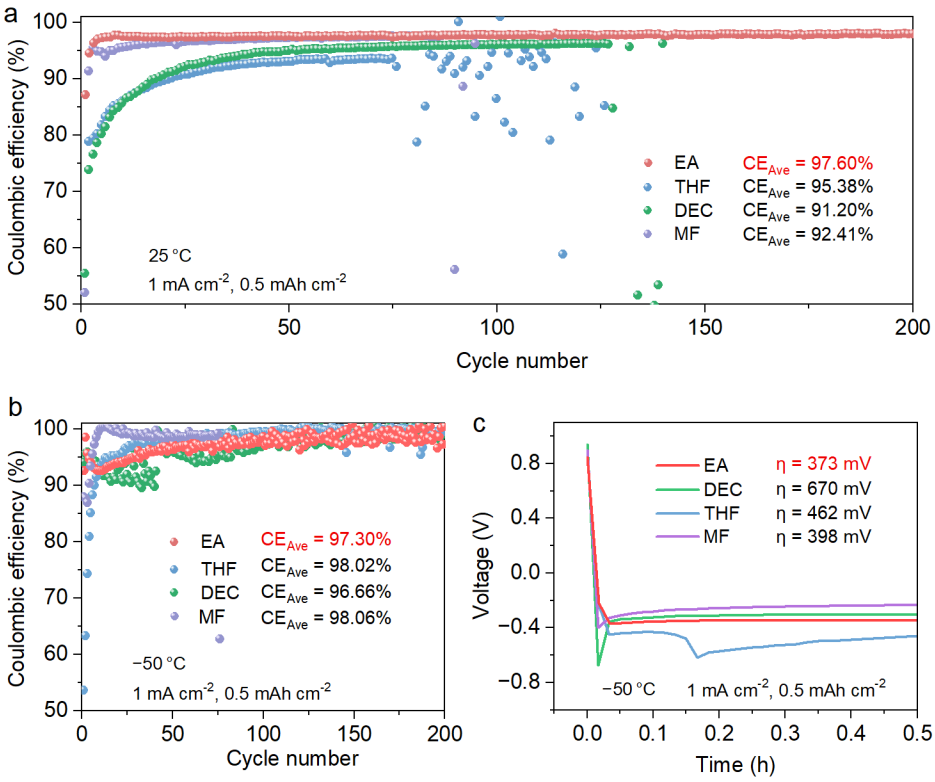

Fig. R3/ Supplementary Fig. 2 a, b The CEs of Zn||Cu batteries at a current density of 1 mA cm^{-2} and 0.5 mAh cm^{-2} at 25 °C (a) and −50 °C (b). c, The first discharge curve of Zn||Cu batteries at a current density of 1 mA cm^{-2} and an areal capacity of 0.5 mAh cm^{-2}.

Comment 5. In the sentence "Electrostatic portion of the metallic lithium is zero for both sides, as it is electrically neutral," the mention of metallic lithium appears to be inconsistent with the rest of the manuscript, which focuses on zinc-based systems. This seems to be an oversight or a typographical error. Please revise it accordingly to maintain accuracy and consistency in terminology throughout the manuscript.

Response: Thank you for reminding us of this. We have revised this section in the Supplementary Discussion on page 1 in Supplementary Information:

"Electrostatic portion of the metallic zinc is zero for both sides, as it is electrically neutral."

Comment 6. There appears to be a clear error in Fig. 1d regarding the DN of water. According to Gutmann's widely cited work (Gutmann, V. "Empirical parameters for donor and acceptor

properties of solvents." Electrochimica Acta 21.9 (1976): 661-670.), the donor number of liquid water is approximately 33, not 18, which corresponds to the gas phase. Please revise the value accordingly to ensure consistency with established empirical data.

Response: Thank you for catching this; we fixed the donor number of liquid water to 33. (Figure 1d and Supplementary Table 1)

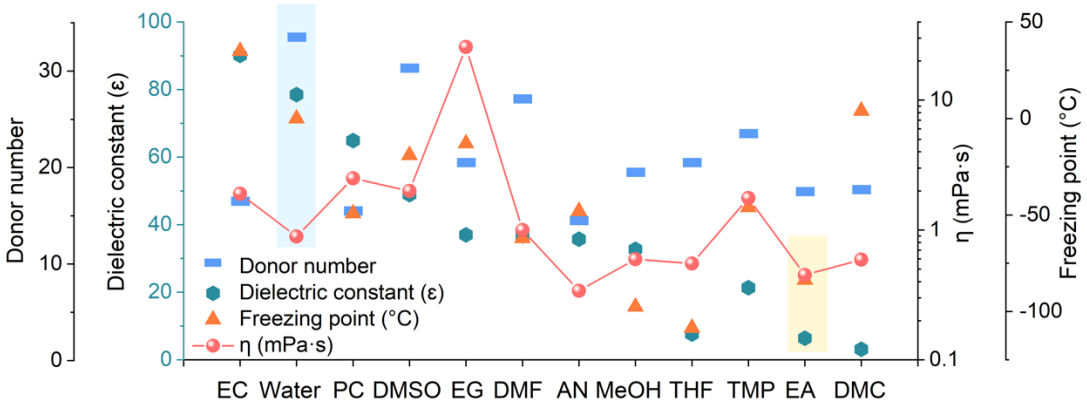

Fig. R4/Fig. 1 Comparison of solvent properties, including donor number, dielectric constant, freezing point, and viscosity.

Supplementary Table 1. Comparison of solvent properties, including donor number, dielectric constant, freezing point, and viscosity.

Solvent	Donor number	Freezing point (°C)	η (mPa·s)	ε
EA	**17.2**	**−83.6**	**1.9**	**6.4**
PC	15.0	−49.2	2.5	64.9
DMSO	29.8	−19.0	2.0	48.9
EG	20.0	−12.9	25.66	37.0
DMF	26.6	−62.0	1.0	36.7
AN	14.0	−48.0	0.34	35.7

MeOH	19.0	−97.5	0.59	32.7
THF	20.0	−108.5	0.55	7.4
TMP	23.0	−46.0	1.76	21.3
DMC	17.2	4.0	0.59	3.1
EC	16.0	35.0	1.90	90.1
H_2O	**~33.0**	**0**	**0.85**	**78.46**

Comment 7. The authors screened the optimal electrolyte formulation based on ionic conductivity derived from EIS measurements. However, no corresponding chronoamperometry data and EIS fitting results are provided. According to previous studies (Yang, Jin-Lin, et al. "Designing single-ion conductive electrolytes for aqueous zinc batteries." Matter 7.6 (2024): 1928-1949.), the impedance of aqueous Zn-ion batteries can be unstable. Therefore, for ionic conductivity measurements at different temperatures, we recommend the use of a conductivity meter to obtain more reliable and reproducible results. Moreover, based on the data presented, the ionic conductivity of the 20(H_2O):1(EA) electrolyte is comparable to that of the 16:1 formulation across various temperatures. Therefore, selecting 16:1 as the optimal concentration requires further justification, such as by comparing Coulombic efficiency, symmetric cell lifespan, or other electrochemical performance metrics.

Response: Thank you for the comment. The suggestion has helped us enhance our manuscript. Accordingly, we measured the ionic conductivity at different temperatures using a conductivity meter (Mettler Toledo Conductivity Meter, FE38-Standard) and included this information in Supplementary Fig. 6 and Supplementary Table 4. In the revised manuscript, the corresponding conductivity values have been changed on page 5, line 142:

"Among the tested EA:H_2O ratios, 1:16 delivered the highest ionic conductivity at −50 °C (24.92 mS cm^{-1})."

In addition, we compared the Coulombic efficiency of various electrolytes and the lifespan of symmetric batteries. We have added this data as a new Supplementary Fig. 7. The corresponding explanations were also added in the Supplementary Note 5 (Page 10 in Supplementary information):

"Zn||Cu asymmetric cells were assembled to assess Zn plating/stripping reversibility across EA:H_2O ratios from 0:1 to 1:6. As shown in Supplementary Fig. 7a,b, the MDCE (EA:H_2O = 1:16) delivered average Coulombic efficiencies of 98.2% at 25 °C and 97.14% at -50 °C, outperforming the other formulations. In contrast, the HDCE (0:1) exhibited an operational life of only ~100 cycles with an average Coulombic efficiency of 43.34% and failed to operate at -50 °C.

Symmetric Zn||Zn cells were then used to probe cycling stability (Supplementary Fig. 7c-e). Most EA-containing electrolytes showed markedly enhanced stability relative to 0:1 and 1:20 ratios. Notably, in the MDCE cell the overpotential decreased from 92.6 mV (0-10 h) to 21.1 mV (90-100 h), consistent with the formation of a stable, ion-conductive SEI during initial cycles. These results identify EA:H_2O = 1:16 as the optimal composition for MDCE."

And a summary has been provided in the main text. on page 6, line 147:

"To assess zinc plating/stripping reversibility across compositions, we assembled Zn||Cu and Zn||Zn cells at 25 °C and −50 °C; both experiments identified EA:H_2O = 1:16 as the optimal ratio for low-temperature operation (Supplementary Fig. 7; Supplementary Note 5)."

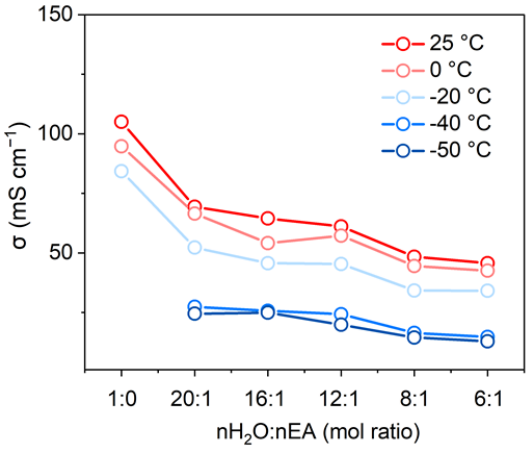

Fig. R5/Supplementary Fig. 6 The ionic conductivities of $Zn(ClO_4)_2$ in H_2O/EA solutions with different H_2O/EA molar ratios from 1:0 to 6:1 at different temperatures test by conductivity meter (The conductivity of the electrolyte at 25, 0, −20, −40, and −50°C was measured using the Mettler Toledo Conductivity Meter (FE38-Standard)).

Supplementary Table 4. Temperature-dependent ionic conductivity of 2 M $Zn(ClO_4)_2$ in H_2O/EA across EA:H_2O ratios from 0:1 to 1:6, measured with a conductivity meter.

Electrolytes	σ (mS cm^{-1})				
EA:H_2O molar ratios	25 °C	0 °C	-20 °C	-40 °C	-50 °C
0:1	105.01	94.78	84.28	--	--
1:20	69.37	66.5	52.22	27.37	24.5
1:16	64.47	54.11	45.71	25.69	24.92
1:12	61.11	57.26	45.36	24.29	19.88
1:8	48.37	44.52	34.23	16.45	14.49
1:6	45.71	42.56	34.09	14.7	12.88

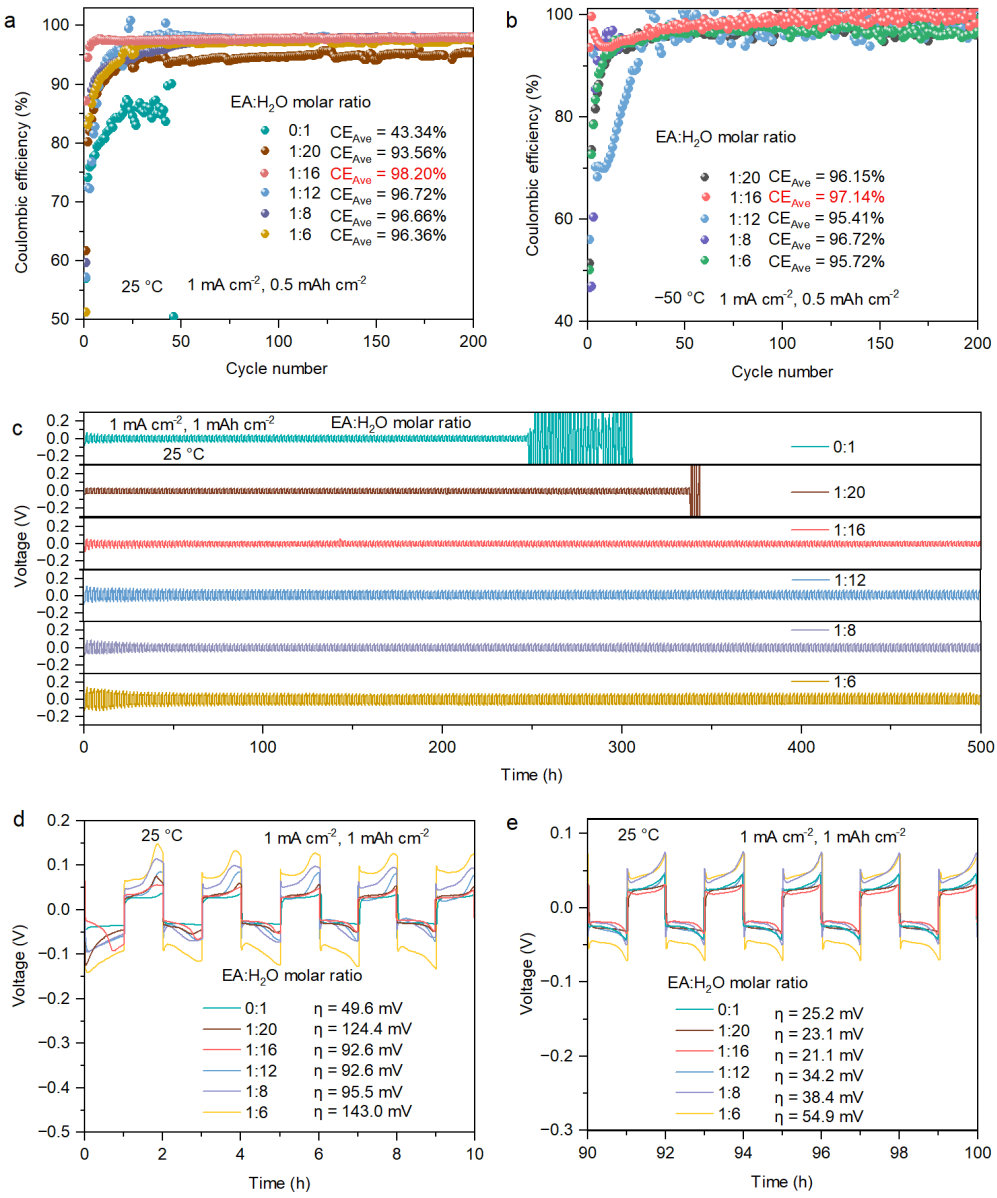

Fig. R6/Supplementary Fig. 7 a, b The CEs of Zn||Cu batteries at a current and capacity density of 1 mA cm^{-2} and 0.5 mAh cm^{-2} at 25 °C (a) and −50 °C (b). c-e, The cycling performance of Zn||Zn batteries at a current and capacity density of 1 mA cm^{-2} and 1 mAh cm^{-2} (c), and local time voltage curve within 0-10 hours (d) and 90-100 hours (e).

Comment 8. The authors provided WT-EXAFS data in Fig. 2c, effectively visualizing the EXAFS signals. However, for rigorous validation and clarity of EXAFS fitting results, the authors are requested to also provide the original Zn K-edge EXAFS oscillation data (in k-space) and the

corresponding fitting curves in R-space. Specifically, please include plots clearly showing the experimental and fitted EXAFS data overlaid in both k-space and R-space, along with a detailed summary table of structural parameters (coordination number, bond length, etc.). This information is essential for ensuring transparency, reproducibility, and robust evaluation of the EXAFS analysis.

Response: Thank you for the comments. According to the reviewer's suggestion, we added plots showing the experimental and fitted EXAFS data overlaid in both k-space and R-space, along with a detailed summary table of structural parameters (coordination number, bond length, etc.) of all samples in the supplementary information. As shown in Supplementary Fig. 10 and Supplementary Table 5. Therefore, we have corrected the writing to make it more concise and accurate on page 7, line 185:

"To resolve the Zn^{2+} solvation structure, we compared experimental XAFS with spectra simulated from DFT-optimized models of $[Zn(ClO_4)(H_2O)_5)]^+$ and $[Zn(ClO_4)EA(H_2O)_4]^+$ (Supplementary Fig.10a-f). In the EXAFS region, a pronounced peak at 1.65 Å corresponds to the Zn–O distance in $[Zn(ClO_4)(H_2O)_5)]^+$ complex[32]. By contrast, MDCE exhibits enhanced multi-shell features, indicating a more heterogeneous coordination environment. Wavelet-transform EXAFS further separates these environments and reveals additional high-k components in MDCE attributable to EA/ClO_4^- coordination (Fig. 2c; Supplementary Fig. 10g)."

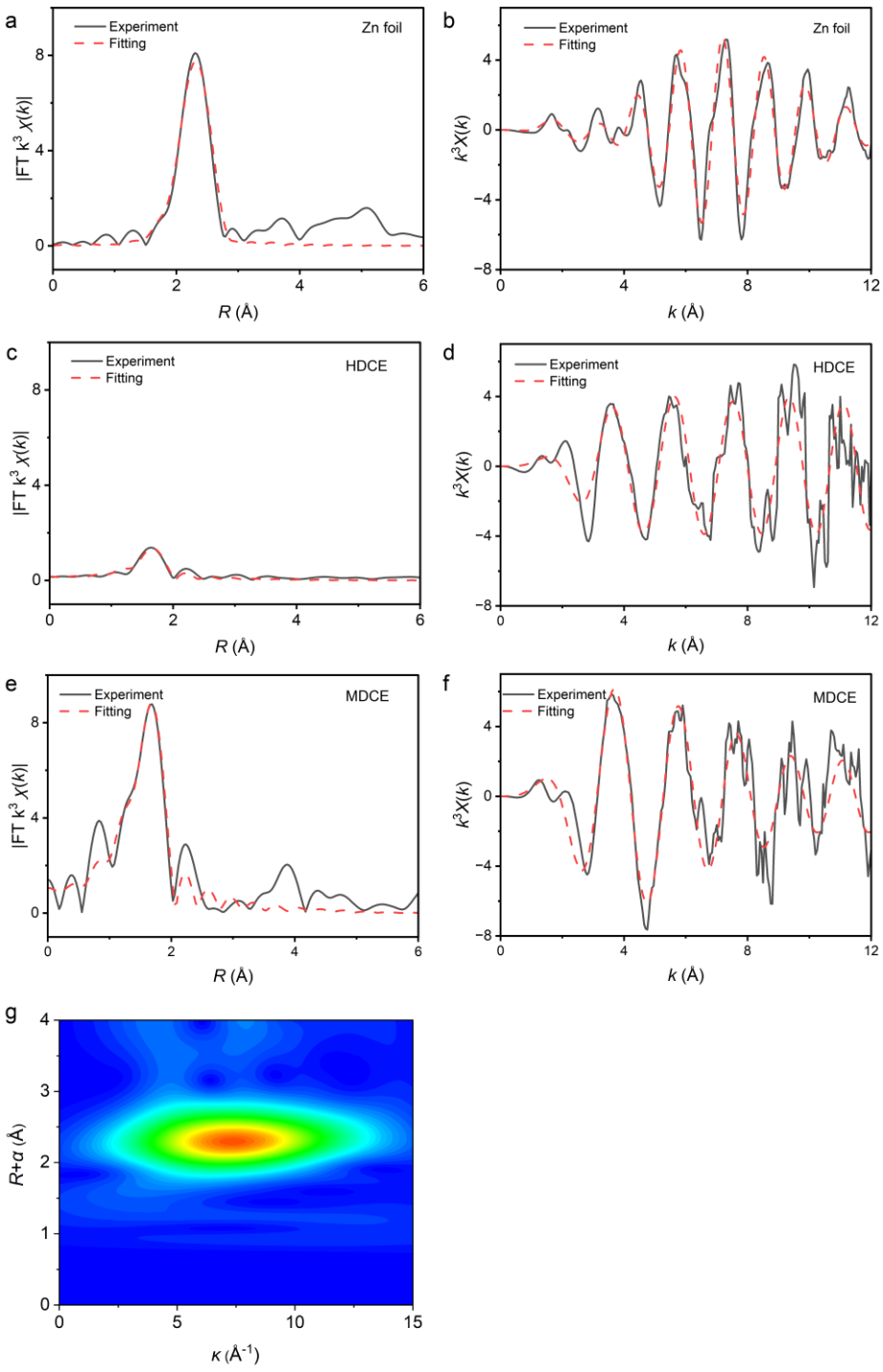

Fig. R7/Supplementary Fig. 10 a, b Fitting of EXAFS spectra in R space (a) and k space (b) for Zn foil. c, d, e, f Fitting of EXAFS spectra in R space and k space for HDCE based on DFT optimized molecular geometries of $[Zn(ClO_4)(H_2O)_5]^+$ (c, d) and MDCE based on DFT optimized molecular geometries of $[Zn(ClO_4)EA(H_2O)_4]^+$ (e, f). (g) Wavelet transforms for the Zn foil.

Supplementary Table 5. Curve-fitting parameters for Zn K-edge EXAFS of $Zn(H_2O)_5(ClO_4)^+$ and $Zn(H_2O)_4EA(ClO_4)^+$standards. Reported parameters: coordination number (C.N.), bond distance (R), Debye–Waller factor (σ^2), inner potential correction (ΔE_0), and R-factor (goodness of fit). S_0^2 was fixed at 0.85.

Sample	Path	R (Å)	C. N.	$\sigma^2\times10^3$ ($Å^2$)	ΔE_0 (eV)	R factor
Zn	Zn-Zn	2.64	6	12.9	−0.038	0.009
HDCE (path in $Zn(H_2O)_5(ClO_4)^+$)	Zn-O (H_2O)	2.13	5.1	6.4	−1.8	0.007
	Zn-O (ClO_4)	2.09	0.9			
MDCE(path in $Zn(H_2O)_4EA(ClO_4)^+$)	Zn-O (H_2O)	2.13	3.4	9.6	−2.6	0.013
	Zn-O (ClO_4)	2.09	1.5			
	Zn-O (EA)	2.15	1.1			

Comment 9. The description of the in situ FTIR difference spectra is quite confusing. First, it is unclear whether the spectra shown in Fig. 3c and Fig. S14b correspond to HDCE or MDCE, the manuscript does not clarify this, leaving the reader uncertain. Second, the definitions of $A(t_x)$, $A(t_0)$, and $A(t_z)$ are not provided in the main text, and to the best of my knowledge, these are not standard or widely recognized terms. In Fig. S14c and d, there is also a clear inconsistency between the y-axis label and the figure captions. The axis label reads "$A(t) - A(t_0)$", while the caption refers to "$A(t_z) - A(t_0)$", which are not equivalent concepts based on the definitions implied in the manuscript. This inconsistency is confusing and should be corrected to ensure clarity. Moreover, according to the authors, $A(t_z)$ represents the first spectrum collected after applying current and should therefore be time-independent. However, the spectral changes shown in the figure appear to vary over time, which contradicts that definition. Additionally, the observed enhancement of W-H relative absorbance for MDCE under biased potential deviates from previous reports in the literature (Yu, Xiaoyu, et al. "Unlocking dynamic solvation chemistry and hydrogen evolution mechanism in aqueous zinc batteries." Journal of the American Chemical Society 146.25 (2024): 17103-17113.). The authors should provide a clear explanation for this discrepancy. Lastly, important experimental details are missing, such as the duration of the charge/discharge process,

spectral acquisition resolution, and the number of scans. Providing this information is necessary for readers to fully understand and evaluate the experimental setup and results.

Response: Thank you for your comments. We will address them below one by one.

First, we reorganized the content and logic to make the connection between images and samples clearer. Specifically, we added the following text to the manuscript on page 10, line 269:

"In MDCE, significant spectral changes occurred during the initial discharge/charge cycle, including bands related to decomposition and species formation for interfacial H_2O (νOH), EA (νCH_3, νOCH_2), and ClO_4^- (νClO) (Fig. 3e). These changes illustrate the dynamics of weak hydrogen bonds (W-H) and strong hydrogen bonds (S-H) of interfacial water, that is water at the interface between the electrode surface and the electrolyte solution (Fig. 3f). In HDCE, the increase in W-H signal during plating indicates higher water activity and stronger HER (Supplementary Fig. 16b)."

Second, we redefined the acquired spectral information and supplemented the experimental details in the method part on page 22, line 585:

"Background spectra were first recorded in air, followed by $A(t_0)$ after electrolyte filling (open circuit) and time-resolved spectra $A(t_x)$, $A(t_y)$ under current. Relative absorbance was defined as $\Delta A(t_x)=A(t_x)-A(t_0)$ (abrupt change under bias) and $\Delta A(t_y)=A(t_y)-A(t_x)$ (subsequent gradual evolution) (Fig. R8)."

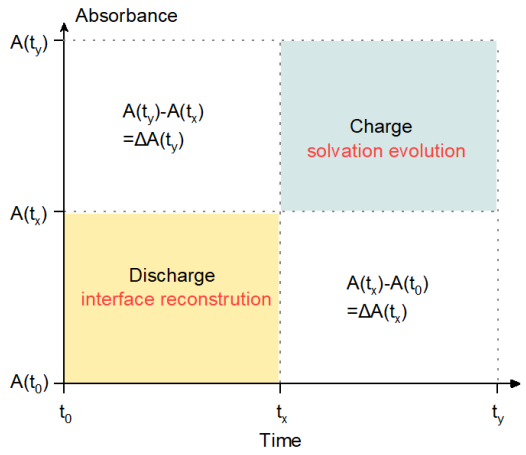

Fig. R8 The dynamic interface evolution during Zn plating/stripping. The process can be decoupled into two stages, abrupt change of interface reconstruction (expressed as $\Delta A(t_x) = A(t_x) - A(t_0)$) and gradual change of (de)solvation evolution (expressed as $\Delta A(t_y) = A(t_y) - A(t_x)$)[56].

[56] Yu, X. et al. Deciphering multi-dimensional interfacial mechanisms via organic cosolvent engineering for sustainable zinc metal batteries. *Nat. Commun*. **16**, 3820 (2025).

During infrared spectroscopy testing, the high humidity in the laboratory significantly influenced the infrared absorption peaks of water molecules, causing a continuous rise in water peak intensity. To reduce environmental humidity's effects on the results, controlled humidity chamber was employed to lower humidity below 10%. Under these controlled conditions, it was observed that during charging, the infrared absorption intensity of the weak hydrogen bond (W-H) increased, whereas during discharging, this peak's intensity noticeably decreased (Fig. R9).

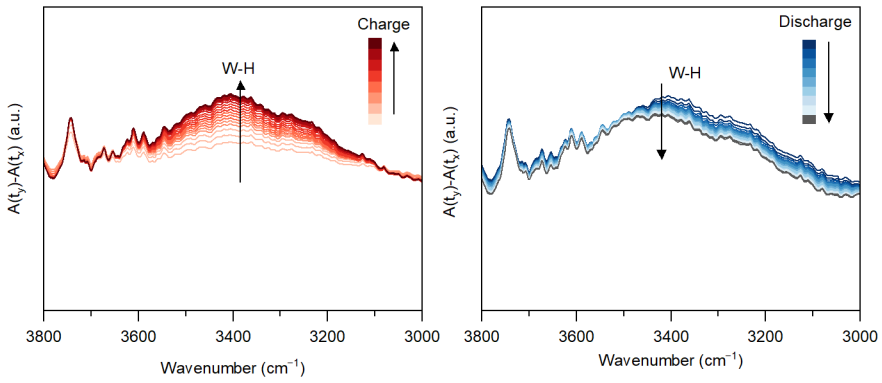

Fig. R9 The $A(t_y)$-$A(t_x)$ relative absorbance evolution during charging (left, red) and discharging (right, blue), which depicts the evolution of W-H stretching vibration of interfacial H_2O in MDCE.

Lastly, we supplemented the experimental details in the methods section and modified the manuscript accordingly on page 22, line 579:

"*In situ* electrochemical FTIR was performed on a Vertex 70 spectrometer (Bruker) coupled to a CHI760E workstation (Shanghai Chinstrument Co., Ltd.) and equipped with a liquid-nitrogen-cooled broadband MCT detector (Beijing bjscistar Co., Ltd.) at room temperature. Spectra were collected in absorbance mode [$A = -\log(I/I_0)$] at a fixed 60° incidence and 4 cm^{-1} resolution. A custom spectro-electrochemical cell used a Cu-mesh working electrode and Zn foil

as both counter and reference; Zn was plated at 0.5 mA for 900 s and stripped at 0.5 mA to a 0.5 V cut-off. Background spectra were first recorded in air, followed by $A(t_0)$ after electrolyte filling (open circuit) and time-resolved spectra $A(t_x)$, $A(t_y)$ under current. Relative absorbance was defined as $\Delta A(t_x)=A(t_x)-A(t_0)$ (abrupt change under bias) and $\Delta A(t_y)=A(t_y)-A(t_x)$ (subsequent gradual evolution).

Comment 10. Why does MDCE exhibit a significantly higher nucleation overpotential difference at −40°C compared to −50°C in Figure 4d?

Response: Thank you for flagging this discrepancy. We repeated the nucleation measurements at −40 °C and −50 °C using a stricter protocol (identical cell history, extended thermal equilibration, and standardized pre-conditioning) across independent cells. The corrected data show that the nucleation overpotential in MDCE is smaller in magnitude at −40 °C than at −50 °C, as expected from transport-limited nucleation kinetics at lower temperature. We have replaced Fig. 4d with the corrected results (and included the corresponding response figure), added representative voltage–time traces with error bars, and updated the Methods to detail the revised protocol so that the outcome is reproducible.

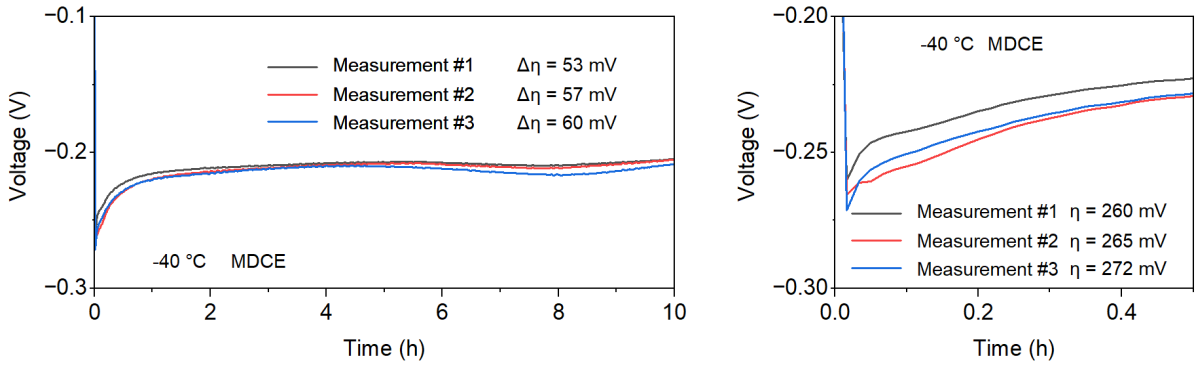

Fig. R10 The nucleation overpotential (η) and the plateau overpotential (Δη) at 0.5 mA cm^{-2} in MDCE at −40°C.

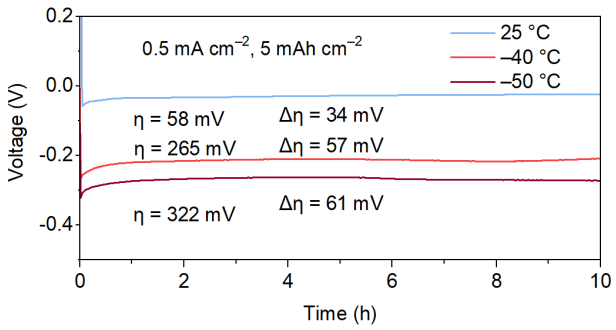

Fig. R11/Figure 4d The nucleation overpotential (η) and the plateau overpotential (Δη) at 0.5 mA cm^{-2} in MDCE at 25°C, −40°C, and −50°C.

Reviewer #2

Comments (major strengths):

The paper reports a dielectric constant modulation strategy to improve the cryogenic performance of aqueous Zn metal batteries. By introducing a low-ε co-solvent (ethyl acetate, EA) into a $Zn(ClO_4)_2$ electrolyte, the authors successfully disrupt the hydrogen-bonding network of water, regulate Zn^{2+} solvation structure, and enable stable Zn plating/stripping under extreme cold conditions (down to –50 °C).

The study is thorough, well-executed, and presented. The approach is novel, and the conclusions are convincingly supported by complementary experimental and simulation data. The electrochemical results are outstanding, especially the symmetric Zn||Zn cycling for over 4,000 h at −50 °C and 10,000 cycles in PANI||Zn full cells.

The manuscript is generally well-organized and experimentally comprehensive. However, the following concerns should be addressed before publication.

Response: Thank you very much for your positive comments and words of praise.

Comment 1. Mechanistic ambiguity in "altering dielectric response" The statement "$Zn(ClO_4)_2 \cdot 6H_2O$ enhances the miscibility of EA and water by altering the solution's overall dielectric response" (page 5, paragraph 1) lacks sufficient mechanistic explanation. While it is suggested that the salt improves solvent compatibility, the phrase "altering dielectric response" remains vague. It would be helpful to clarify how $Zn(ClO_4)_2 \cdot 6H_2O$ influences the dielectric environment — for instance, by coordinating with water to reduce its effective polarity, by screening unfavorable interactions between EA and H_2O, or by modifying hydrogen bonding networks. A brief discussion or reference to a specific interaction model (e.g., salt-mediated dipole alignment or suppression of phase separation) would strengthen this point and aid the reader's understanding.

Response: Thank you for the helpful comment. We have replaced the phrase "altering dielectric response" with a mechanism-based explanation. In brief, $Zn(ClO_4)_2(H_2O)_6$ modulates the local permittivity and improves EA–H_2O miscibility through two coupled effects. First, Zn^{2+} coordinates water to form $[Zn(H_2O)_6]^{2+}$, which decreases the population of strongly hydrogen-bonded, highly polar free water and its orientational polarization. Second, the weakly coordinating, chaotropic ClO_4^- anion disrupts the water hydrogen-bond network and screens unfavorable EA–H_2O dipole interactions. The combined outcome is a lower effective permittivity, weaker dipole–dipole correlations, and a reduced free-energy penalty for mixing. We now state this mechanism in the expanded Supplementary Discussion 2 with a concise interaction-model rationale (ion–ion, ion–dipole, dipole–dipole) framed in the Kirkwood–Frohlich picture of dielectric response, together with supporting literature (Hou et al., Adv. Energy Mater. 2023; Chen and Zhang, Acc. Chem. Res. 2020).

The article has been revised in Supplementary Information on page 2:

"To rationalize the structure–activity relationship of the electrolyte, we introduce classical models for the principal intermolecular interactions (ion–ion, ion–dipole, and dipole–dipole). Their orientation-averaged potential energies are given by Eqs. (7)–(9) (SI units suppressed for clarity)[4,5].

$$U_{ion\text{-}ion} = -\frac{1}{4\pi\varepsilon}\frac{z_1 z_2 e^2}{r} \quad (7)$$

$$U_{ion\text{-}dipole} = -\frac{1}{4\pi\varepsilon}\frac{ze\mu\cos\theta}{r^2} \quad (8)$$

$$U_{dipole\text{-}dipole} = -\frac{1}{(4\pi\varepsilon)^2}\frac{2\mu_1^2\mu_2^2}{3k_B T r^6} \quad (9)$$

The dielectric constant ε quantifies the response to an applied field and arises microscopically from dipole orientation. In a simple mean-field picture, it scales with the effective molecular dipole moment and the number density of dipoles:

$$\varepsilon \propto \frac{\mu_1^2\mu_2^2}{k_B T} \quad (10)$$

Here, U denotes the interaction energy, ε is the dielectric constant, ze is the charge of the ion, μ is the dipole moment of the dipole, r is the distance between ions or the centers of dipoles, θ is the dipole angle relative to the line joining the ion and the center of the dipole, k_B is the Boltzmann

constant, and T is the absolute temperature.

Electrolytes modify dielectric behavior through coordination and network effects. For example, Zn^{2+} forms $[Zn(H_2O)_6]^{2+}$ complexes, binding water and reducing the number density of free water dipoles, thereby lowering their dielectric contribution. At 25 °C, pure water has ε = 78.46[6], whereas a $Zn(ClO_4)_2$ aqueous solution exhibits epsilon ~ 45. In mixed EA/H_2O electrolytes, EA engages in dipole–dipole interactions with water, and the chaotropic anion ClO_4^- disrupts the water hydrogen-bond network. Both effects increase orientational disorder, reduce the effective vector sum of water dipoles, and diminish the bulk dielectric response. The resulting local dielectric shielding, integrated over the liquid, decreases the overall ε. (Page 2, Supplementary information)

[4] R. Hou, S. Guo, H. Zhou, Atomic insights into advances and issues in low-temperature electrolytes. *Adv. Energy Mater.* 2023, 13, 2300053.

[5] Chen, X. & Zhang, Q. Atomic insights into the fundamental interactions in lithium battery electrolytes. *Acc. Chem. Res.* 2020, 53, 1992-2002.

Comment 2. Spectral interpretation lacks quantification or deconvolution The FTIR and Raman shifts (e.g., C–O–C from 1046 to 1040 cm^{-1}, O–Cl–O from 1079 to 1073 cm^{-1}) are invoked as evidence of solvation changes, but the authors present only qualitative discussion. There is no spectral deconvolution or integration data (e.g., peak area ratios) to quantify solvation shell reorganization or binding strength. Especially for the ClO_4^- shift, which is subtle, a clearer attribution is needed—could the observed change be due to simple dilution, not coordination? A deeper spectroscopic analysis would strengthen the claims.

Response: Thank you very much for your valuable suggestions. We conducted quantitative deconvolution of infrared band to investigate and quantify the solvation shell reorganization focusing on the C–O–C from 1046 to 1040 cm^{-1} and O–Cl–O from 1079 to 1073 cm^{-1}. CIP band area increases from 16% to 21.9% on adding EA, SSIP decreases from 49.5% to 43.3% (Supplementary Fig. 7d). Spectra were baseline-corrected and fitted with Voigt profiles using shared-width constraints; peak positions, FWHM, and integrated areas were extracted. Furthermore, the following was added to the manuscript in order to explain this analysis in main text on page 6, line 162:

"To elucidate ion pairing in the MDCE, we probed Zn^{2+}–ClO_4^-coordination by FTIR (Supplementary Fig. 8c,d). The results showed peaks assigned to solvent-separated ion pairs (SSIP, noncoordinated ClO_4^-, 1076 cm^{-1}), contact ion pairs, (CIPs, Zn-$(ClO_4^-)_{n\geq1}$, 1047 cm^{-1}), indicating strong adsorption for ClO_4^-, free anion (1114 cm^{-1}) and free EA (1037 cm^{-1}). Upon EA addition, the SSIP and free-anion bands diminish while the CIP band grows, indicating strengthened cation–anion association with a fraction of EA remaining uncoordinated (Supplementary Fig. 8c,d)."

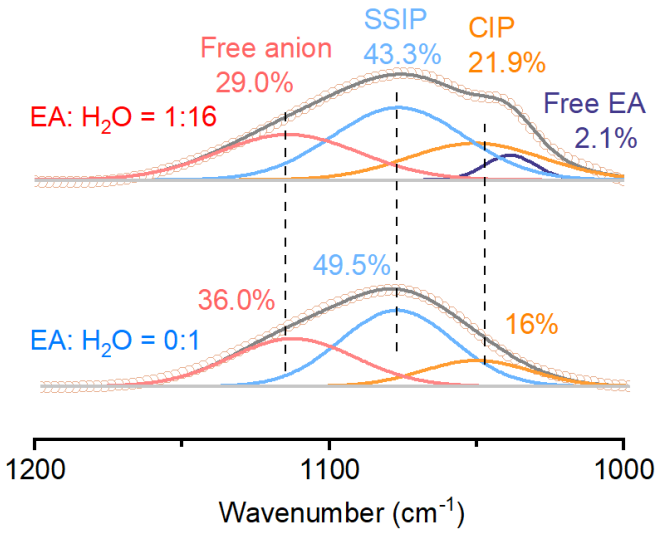

Fig. R12/Supplementary Fig. 8d Deconvolution result of FTIR spectra for 2 M $Zn(ClO_4)_2$ H_2O (EA: H_2O = 0:1) and 2 M $Zn(ClO_4)_2$ EA:H_2O (EA:H_2O = 1:16) electrolytes at 1,200–1,000 cm^{-1}.

Comment 3. The authors state that FTIR/Raman results (e.g., shifts in O–H vibrations) "promote the conversion of weak and medium-strength hydrogen bond networks to strong hydrogen bond networks," which contradicts the usual interpretation that the addition of organic co-solvents weakens water's H-bond network. The use of "strong H-bond network" here needs clarification: does this imply localized but fewer, stronger H-bonds or just a spectral artifact? Otherwise, the interpretation appears inconsistent to disrupt water structure to improve low-temperature performance.

Response: Thank you for bringing the problem to our attention. As you mentioned, we have corrected our inaccurate descriptions based on the results of Raman and infrared analysis. Both FTIR and Raman indicate progressive weakening of the water H-bond network with EA:

cluster/bulk-water O–H bands shift to higher wavenumber while the non–H-bonded component grows (to ~60% at EA:H_2O=1:6), consistent with reduced ordering at low temperature (Main Fig. 2a; Supplementary Fig. 9)

We have corrected this statement in the main text on page 7, line 176:

"These results suggest an increased disruption of the hydrogen-bonding network of water and promote the conversion of weak and strong-strength hydrogen bond networks to non-hydrogen bond networks in water, which potentially inhibits the ordered arrangement of water molecules induced by a decrease in temperature."

Comment 4. The potentiometric measurement of solvation energy (OCP between asymmetric electrolytes) is elegant, but its accuracy depends on minimizing liquid junction potential and assuming identical Zn activity at both electrodes. While Supplementary Discussion 1 outlines these assumptions, no control (e.g., symmetric electrolyte test, or multiple Zn salts) is shown to validate the result.

Response: Thank you for the thorough review. We supplemented the experiments and conducted further analysis based on your suggestions, which are included in Supplementary Fig. 13 and Supplementary Table 6. We supplemented with symmetric electrolyte testing to verify that the Zn activity of the two electrodes is the same under minimized liquid junction potential. When the reference electrolyte and the test electrolyte are the same, the potential remains around 0 V. The measured potential ensures that it only reflects the electrode reactions themselves, eliminating the impact of additional potentials at the electrolyte interface. In addition, we supplemented with different reference electrolytes to verify the more negative free energy of the MDCE.

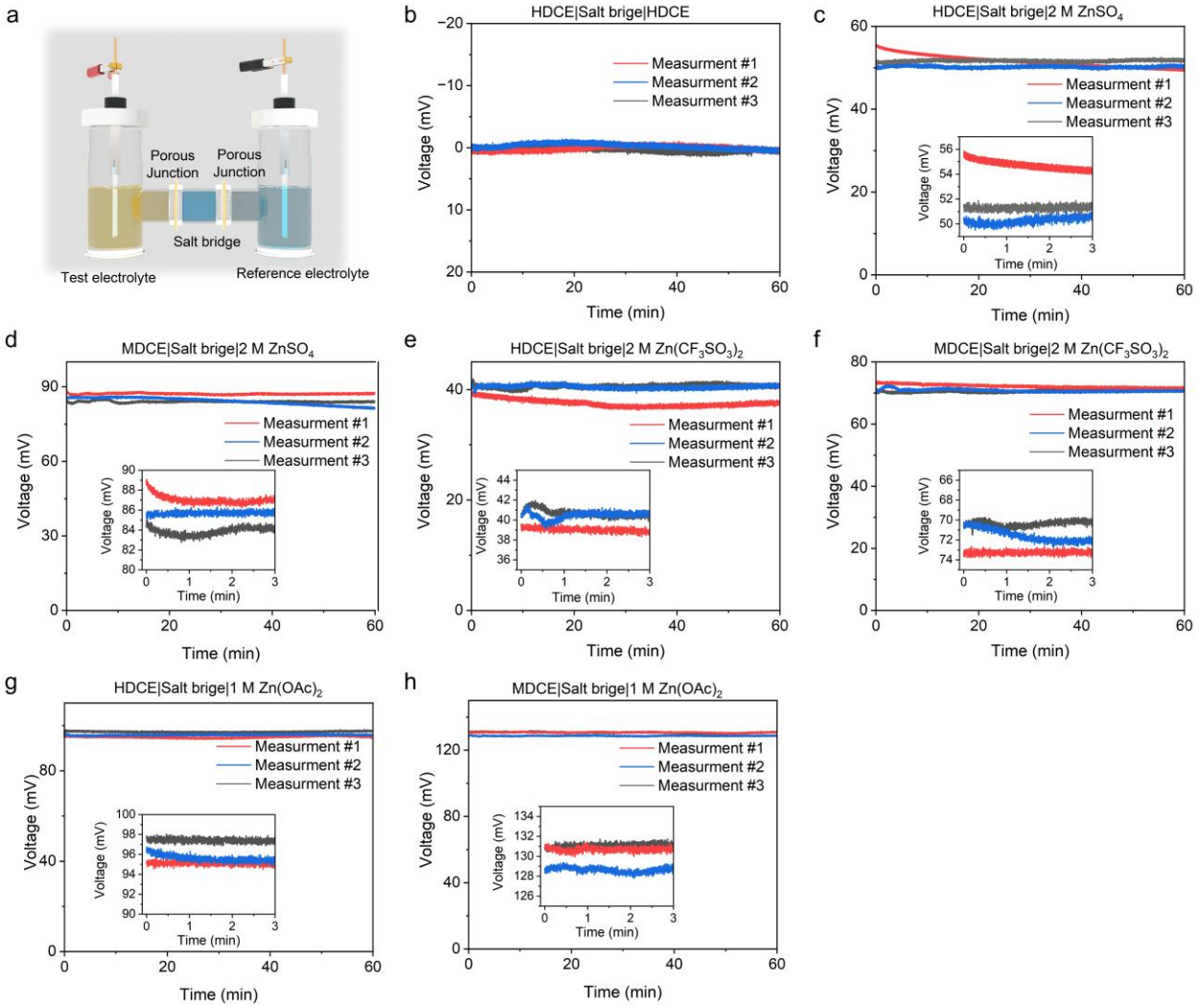

Fig. R13/Supplementary Fig. 13 Potentiometric measurement of relative Zn^{2+} solvation energy. (a) H-cell setup: two Zn electrodes, each immersed in a different electrolyte, a reference electrolyte (EL_{ref}) and a test electrolyte (EL_{test}). The open-circuit cell voltage E_cell reports the difference in Zn^{2+} solvation free energy between EL_{test} and EL_{ref} (ΔG = -nFE _cell; see Supplementary Discussion S1). (b) Representative voltage trace for HDCE vs an aqueous reference electrolyte. (c–h) HDCE (c,e,g) and MDCE (d,f,h) measured against 2 M $ZnSO_{4(aq)}$, 2 M $Zn(CF_3SO_3)_{2(aq)}$, and 1 M $Zn(OAc)_{2(aq)}$, respectively. A typical measurement is completed within 3 min with negligible mixing-induced drift; over 60 min, drift is approximately 1–2 mV.

Supplementary Table 6. Summary of solvation energy for each electrolyte.

Solvent	Reference electrolyte	Voltage (V)	Solvation Energy (eV)	Solvation Energy (kJ mol^{-1})
HDCE	HDCE	~0	~0	~0
HDCE	2 M $ZnSO_4$ H_2O	0.0529 ± 0.00017	-0.1058 ± 0.00034	-10.1568 ± 0.0326
MDCE	2 M $ZnSO_4$ H_2O	0.0860 ± 0.00110	-0.1720 ± 0.00220	-16.5954 ± 0.2123
HDCE	2 M $Zn(CF_3SO_3)_2$ H_2O	0.0401 ± 0.00007	-0.0774 ± 0.00014	-7.7381 ± 0.0135
MDCE	2 M $Zn(CF_3SO_3)_2$ H_2O	0.0718 ± 0.00012	-0.1386 ± 0.00232	-13.8552 ± 0.0232
HDCE	1 M $Zn(OAc)_2$ H_2O	0.0960 ± 0.00017	-0.1853 ± 0.00033	-18.5251 ± 0.0328
MDCE	1 M $Zn(OAc)_2$ H_2O	0.1301 ± 0.00009	-0.2511 ± 0.00174	-25.1054 ± 0.0174

Comment 5. The authors propose that stronger Zn^{2+}–ClO_4^- pairing (enabled by lower ε) leads to SEI formation via ClO_4^- reduction. However, in aqueous systems, ClO_4^- is generally inert under standard potentials. No electrochemical or chemical evidence (e.g., cyclic voltammetry, ion chromatography) is provided to confirm ClO_4^- reduction or its conversion to SEI-forming species. Without this, the link between ion pairing and SEI composition remains speculative.

Response: Thank you for this valuable suggestion. We measured the onset of anion reduction by linear sweep voltammetry (LSV) and incorporated the detailed description below verbatim in the manuscript on page 10, line 280:

"Consistent with the FTIR transients pointing to early interphase formation, linear sweep voltammetry differentiates the two electrolytes (Supplementary Fig. 17). The full-scale LSV curves in Supplementary Fig. 17a show the behavior of both electrolytes. As can be seen from the enlarged curves in Supplementary Fig. 17b, the first reduction scan in the HDCE reveals HER starting at −0.86 V, where zinc deposition initiates sharply. In contrast, the first reduction scan in the MDCE includes a distinctive reduction peak starting at −0.71 V, which reaches its maximum at −0.76 V (Supplementary Fig. 17c). The reduction peak can only be observed in the first cycle and disappeared in the second cycle. This phenomenon is a typical signature of SEI formation[44]."

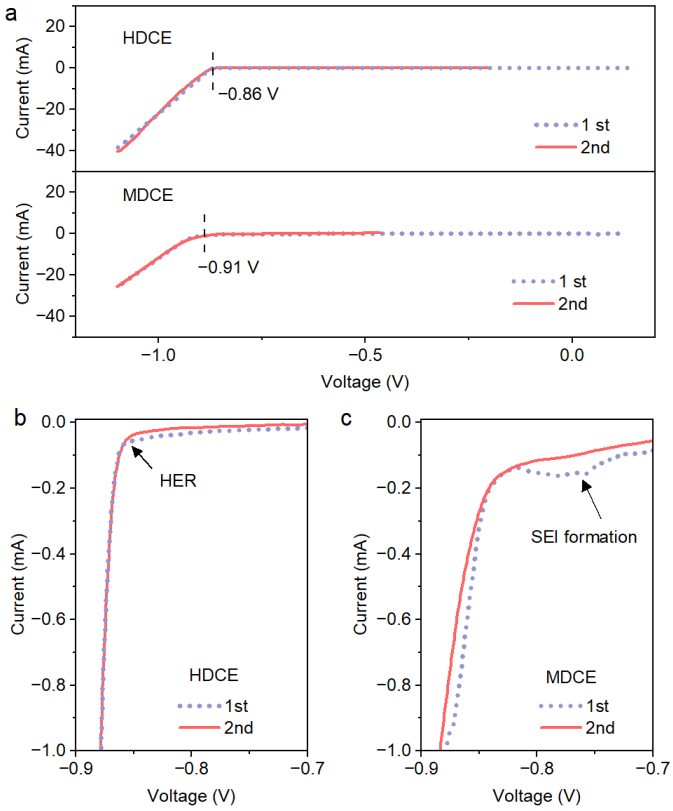

Fig. R14/Supplementary Fig. 17 (a) Full-scale LSV and magnified views for (b) HDCE and (c) MDCE, recorded with Cu foil (working), Zn metal (counter), and Ag/AgCl (reference).

[44] Chen, T., Wang, Y., Li, X., Yuan, T., Pang, Y. & Zheng, S. Enabling solid-electrolyte interphase formation prior to water reduction in aqueous zinc batteries by mild protic chemistry. *Angew. Chem. Inter. Edit.* **64**, e202424642 (2025).

Furthermore, ex situ mass spectrometry of the SEI shows a strong Cl signal with negligible ClO_4^-, indicating consumption of perchlorate to form Cl-containing SEI species (Fig. R15).

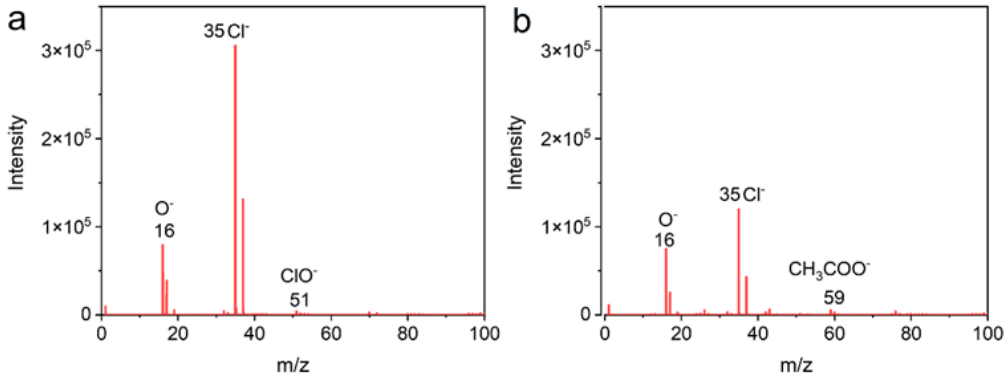

Fig. R15/Supplementary Fig. 29 a,b, Mass spectrometry of cycled Zn anode in HDCE (a) and MDCE (b).

Comment 6. While the manuscript convincingly demonstrates the formation of a robust SEI layer in the MDCE system through cryo-TEM, XPS, and TOF-SIMS analysis, the underlying mechanism by which EA promotes SEI formation remains insufficiently explained. Given the known challenges in forming SEI in aqueous systems due to competitive HER, it is unclear how EA reduction products contribute to SEI nucleation and growth. Additionally, the possible synergistic decomposition of EA and ClO_4^- is not well discussed.

Suggested revision: Please clarify the role of EA in SEI formation at the molecular level. Is there any evidence of EA-derived species (e.g., acetate) directly contributing to SEI structure? Including reaction pathway analysis or DFT simulations would significantly strengthen the mechanistic claims.

Response: Thank you very much for your valuable suggestions. Density functional theory calculations indicate that the downstream reactions resulting from the decomposition of EA are the cause of the formation of organic components in the SEI (Fig. R16/Supplementary Fig. 30). We calculated the reduction pathway for the decomposition of EA using DFT. And we have added the corresponding content in the main text on page 17, line 458:

"DFT indicates that EA undergoes single-electron reduction; the resulting radical/carbanion then deprotonates to an alkene, while acetate (CH_3COO^-) coordinates Zn^{2+} and contributes to forming an organic-rich SEI. The computed reaction free energy for overall decomposition reaction EA $\rightarrow CH_3COO^- + CH_2CH_3$ is -1.12 eV at 298 K and -1.06 eV at 233 K, indicating a thermodynamically favorable pathway that persists at low temperature (Supplementary Fig. 30)"

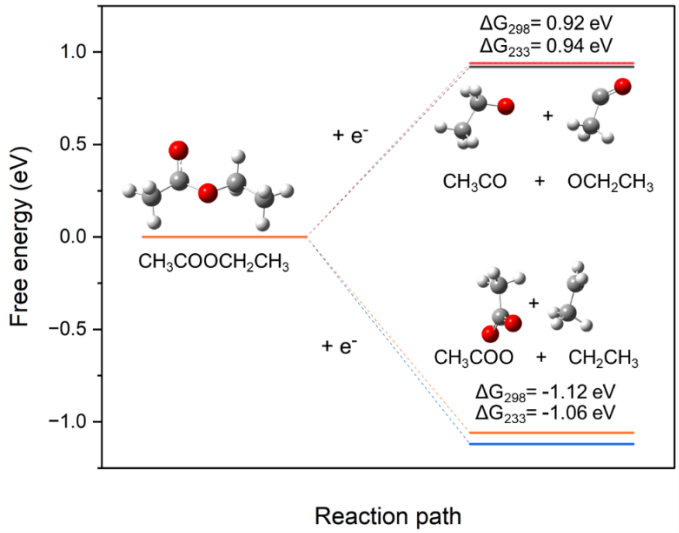

Fig. R16/Supplementary Fig. 30 Calculated reaction energetics (Delta G) for the electron-induced reduction and decomposition of EA.

Computational details are provided in the Methods on page 24, line 656:

Molecular-orbital energies and EA-reduction energetics were computed with Gaussian 16[69] at the M05-2X/6-31++G(d,p) level, using a polarizable-continuum (PCM) water model for solvation[70].

[69] Gaussian 16 rev. C.01 (Wallingford, CT, 2016).

[70] Scalmani, G. & Frisch, M. J. Continuous surface charge polarizable continuum models of solvation. I. General formalism. J. Chem. Phys. 132 (2010).

The distribution results of Cl^- and CH_3COO^- in TOF-SIMS indicate that both ClO_4^- and EA have been decomposed. The presence of the C-Cl peak in XPS suggests a possible synergistic decomposition of EA and ClO_4^-. According to your suggestion, we further discussed the promoting effect of EA addition on anion decomposition. Following this, we employed density functional theory (DFT) calculations to examine the highest occupied molecular orbital (HOMO) and lowest unoccupied molecular orbital (LUMO) energy levels of the primary Zn^{2+} solvation structures and provide the corresponding explanation in the main text on page 8, line 221:

"DFT frontier-orbital analysis shows that EA-containing CIP complexes have a smaller HOMO–LUMO gap than CIPs without EA, implying greater electron-transfer propensity and facilitating anion-derived SEI formation (Supplementary Fig. 11e) [36]."

[36] Hei, P., Sai, Y., Yu, L., Lin, Y., Li, B., Hu, G., Wu, W., Wang, J., Sun, X., Liu, X.-X. & Song, Y. Cosolvent electrolyte design for high-voltage aqueous zinc–sulfur batteries. *J. Am. Chem. Soc.* **147**, 27802-27811 (2025).

Together, these results link EA reduction to acetate formation and to an increased propensity for anion-derived SEI, providing a coherent mechanism for EA-promoted SEI nucleation and growth in MDCE.

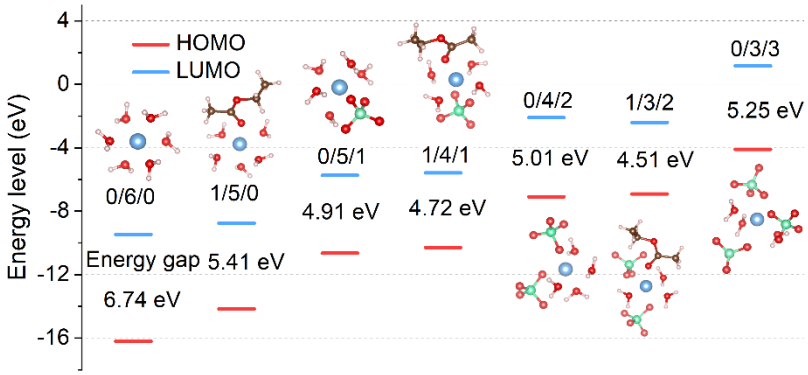

Fig. R17/Supplementary Fig. 11e HOMO/LUMO energy levels and molecular orbitals for solvation structures in HDCE and MDCE; structures are defined by the local fractions of EA/H_2O/ClO_4^-.

Comment 7. The authors attribute Zn corrosion in the HDCE system to Cl^- derived from ClO_4^- decomposition. However, ClO_4^- is generally considered electrochemically inert under standard aqueous conditions, and the manuscript lacks direct evidence for its decomposition. This assertion is critical, as it underpins the comparison between HDCE and MDCE degradation behavior.

Suggested revision: Please provide additional evidence (experimental or theoretical) supporting ClO_4^- decomposition in HDCE. If referencing prior literature, a discussion of the relevant decomposition potential or conditions under which ClO_4^- becomes reactive would improve clarity and credibility.

Response: We agree that additional support research was needed. We now provide converging evidence that perchlorate can be reduced under the strongly cathodic conditions at a Zn surface in

HDCE. First, TOF-SIMS of cycled HDCE anodes shows a pronounced Cl^- signal within the SEI with negligible ClO_4^-, whereas MDCE shows much weaker Cl^- (Fig. R18/Supplementary Fig. 29). XPS also reveals Zn–Cl and a C–Cl component after cycling in HDCE, consistent with chloride-containing interphases. These observations indicate that the chlorine found in the SEI does not originate from trapped undecomposed ClO_4^-.

Taken together, the spectroscopic evidence (TOF-SIMS, XPS) and literature precedent support our assignment that ClO_4^- undergoes reduction to Cl^- in HDCE and contributes to Zn corrosion. We have added this discussion to the main text and cited the operative conditions under which perchlorate becomes reactive

Second, we added a brief literature context on perchlorate reactivity under reducing conditions. Li et al. demonstrated that ClO_4^- participates in the primary solvation sheath of Zn^{2+}, facilitating the in-situ formation of a $Zn_5(OH)_8Cl_2 \cdot H_2O$-rich solid electrolyte interphase (SEI) to suppress the corrosive effect of ClO_4^-. (Li, YS., Geng, LS., Zhang, BM. et al. Concentrated perchlorate-based electrolyte facilitates Zn anode-compatible in-situ solid electrolyte interphase. Rare Met. 44, 950–960 (2025).) Yang et al. also demonstrated the decomposition of ClO_4^-: "Then, these cells were disassembled and the over production of undesired insulating products (i.e., $Zn_4ClO_4(OH)_7$ and $Zn_5(OH)_8Cl_2$) were detected from X-ray diffraction (XRD). (Yang et al., Joule 4, 1557–1574 (2020)).

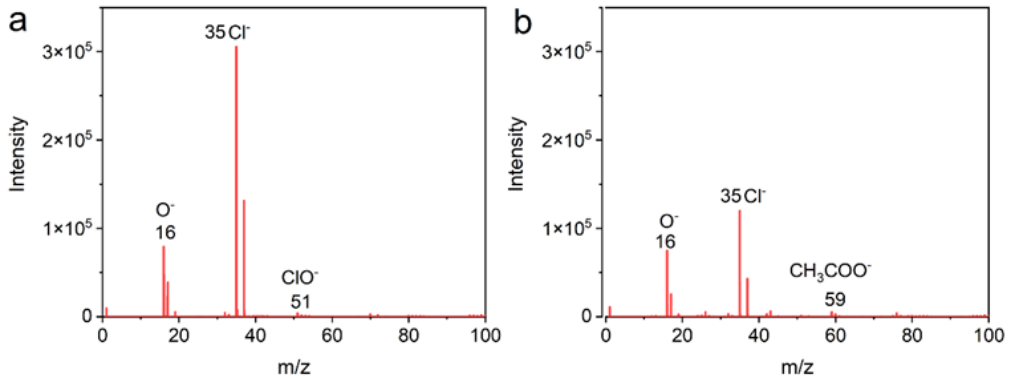

Fig. R18/Supplementary Fig. 29 a,b, Mass spectrometry of cycled Zn anode in HDCE (a) and MDCE (b).

Reviewer #3:

In this work, the author proposed a strategy for low-temperature ZMBs based on tailoring the Zn^{2+} solvation environment by engineering the dielectric constant. Specifically, according to introduction of EA into $Zn(ClO_4)_2$ electrolyte to weaken water's hydrogen-bond network and increase cation-anion pairing. This strategy accelerates Zn^{2+} transport and desolvation, promotes the formation of a protective solid electrolyte interphase rich in organic and inorganic components, and inhibits parasitic hydrogen evolution. Although it achieves excellent electrochemical performance for the cryogenic aqueous zinc batteries, many issues should be addressed before publication.

Response: Thank you very much for your positive comments.

Comment 1. It is mentioned that $Zn(ClO_4)_2 \cdot 6H_2O$ enhances the miscibility of EA and water by altering the solution's overall dielectric response. In the method section, the calculation method and equation of dielectric constants of hybrid salt and solvent (such as $Zn(ClO_4)_2$/EA, $Zn(ClO_4)_2$ EA:H_2O) are not clear. Please supplemented the section.

Response: Thank you for the constructive criticism. To address this criticism, we added the corresponding content to the Methods section of the manuscript on page 24, line 636:

"Dielectric constants of the solvent and electrolytes were calculated using the built-in dielectric analysis module in GROMACS, based on the final 20 ns of the production trajectory[57]. The OPC water model was employed for the simulations known for its high accuracy in dielectric property simulations of aqueous systems[66]. The dipole moment of the system was output every 1000 steps during NVT simulations and used for calculation of dielectric constant." The dielectric constant of liquid electrolytes is calculated according to formula 5[28,29]:

$$\varepsilon = 1 + \frac{< M^2 > - < M >^2}{3\varepsilon_0 V k_B T} \quad (5)$$

where ε is the dielectric constant of specific system, ε the dielectric constant of vacuum, V the volume of the simulation box, k the Boltzmann constant, T the temperature. $M=\sum\vec{\mu}=\sum q\vec{r}$ is the total dipole moment of the system where q and $\vec{r}$ are the charge and position of atoms, respectively. Total dipole moment of the system (M in formula 5) and square of it (M) were both averaged over 5000 frames, which means the dielectric constant is calculated from 5 ns to the end of NVT production run.

[28] Jorgensen, W. L., Maxwell, D. S. & Tirado-Rives, J. Development and testing of the opls all-atom force field on conformational energetics and properties of organic liquids. *J. Am. Chem. Soc.* **118**, 11225-11236 (1996).
[29] Neumann, M. & Steinhauser, O. Computer simulation and the dielectric constant of polarizable polar systems. *Chem. Phys. Lett.* **106**, 563-569 (1984).
[57] Abraham, M. J., Murtola, T., Schulz, R., Páll, S., Smith, J. C., Hess, B. & Lindahl, E. Gromacs: High performance molecular simulations through multi-level parallelism from laptops to supercomputers. SoftwareX 1-2, 19-25 (2015).
[66] Kadaoluwa Pathirannahalage, S. P., Meftahi, N., Elbourne, A., Weiss, A. C. G., McConville, C. F., Padua, A., Winkler, D. A., Costa Gomes, M., Greaves, T. L., Le, T. C., Besford, Q. A. & Christofferson, A. J. Systematic comparison of the structural and dynamic properties of commonly used water models for molecular dynamics simulations. Journal of Chemical Information and Modeling **61**, 4521-4536 (2021).

And we explained how $Zn(ClO_4)_2 \cdot 6H_2O$ affects the dielectric environment to enhance solvent compatibility and supplemented this in Supplementary Discussion 2:

"To rationalize the structure–activity relationship of the electrolyte, we introduce classical models for the principal intermolecular interactions (ion–ion, ion–dipole, and dipole–dipole). Their orientation-averaged potential energies are given by Eqs. (7)–(9) (SI units suppressed for clarity)[4,5].

$$U_{ion\text{-}ion}=-\frac{1}{4\pi\varepsilon}\frac{z_1 z_2 e^2}{r} \quad (7)$$

$$U_{ion\text{-}dipole} = -\frac{1}{4\pi\varepsilon}\frac{ze\mu\cos\theta}{r^2} \quad (8)$$

$$U_{dipole\text{-}dipole} = -\frac{1}{(4\pi\varepsilon)^2}\frac{2\mu_1^2\mu_2^2}{3k_BTr^6} \quad (9)$$

The dielectric constant epsilon quantifies the response to an applied field and arises microscopically from dipole orientation. In a simple mean-field picture, it scales with the effective molecular dipole moment and the number density of dipoles:

$$\varepsilon \propto \frac{\mu_1^2\mu_2^2}{k_BT} \quad (10)$$

Here, U denotes the interaction energy, ε is the dielectric constant, ze is the charge of the ion, μ is the dipole moment of the dipole, r is the distance between ions or the centers of dipoles, θ is the dipole angle relative to the line joining the ion and the center of the dipole, k_B is the Boltzmann constant, and T is the absolute temperature.

Electrolytes modify dielectric behavior through coordination and network effects. For example, Zn^{2+} forms $[Zn(H_2O)_6]^{2+}$ complexes, binding water and reducing the number density of free water dipoles, thereby lowering their dielectric contribution. At 25 °C, pure water has $\varepsilon = 78.46$[6], whereas a $Zn(ClO_4)_2$ aqueous solution exhibits epsilon ~ 45. In mixed EA/H_2O electrolytes, EA engages in dipole–dipole interactions with water, and the chaotropic anion ClO_4^- disrupts the water hydrogen-bond network. Both effects increase orientational disorder, reduce the effective vector sum of water dipoles, and diminish the bulk dielectric response. The resulting local dielectric shielding, integrated over the liquid, decreases the overall ε. (Page 2, Supplementary information)

[4] R. Hou, S. Guo, H. Zhou, Atomic insights into advances and issues in low-temperature electrolytes. *Adv. Energy Mater.* 2023, 13, 2300053.
[5] Chen, X. & Zhang, Q. Atomic insights into the fundamental interactions in lithium battery electrolytes. *Acc. Chem. Res.* 2020, 53, 1992-2002.

Comment 2. The author proposed that EA is an ideal co-solvent because it has a low dielectric constant, low viscosity, and low freezing point. But as can be seen from Table S1, MeOH and THF also have similar characteristics. Besides, other carboxylic esters, such as methyl acetate and methyl formate also have similar characteristics. Why EA was chosen as the co-solvent, the explanation is not sufficient.

Response: Thank you for the comment. We investigated the electrochemical performance of MeOH, THF, and methyl formate (MF) as co-solvents at different temperatures (Fig. R18). Our experimental results (Table S1) demonstrate that the EA-containing electrolyte exhibits significantly higher Coulombic Efficiency (CE) at both room and low temperatures compared to MeOH ($\varepsilon = 32.7$), THF ($\varepsilon = 7.4$) and MF ($\varepsilon = 8.5$), despite their similar physical properties. During the 200 cycles of zinc plating/stripping process, the CE of EA at 25 °C and -50 °C is 97.6% and 97.3% respectively. And the overpotential at -50 °C being 373 mV. This suggests that EA's advantage is not solely determined by dielectric constant or viscosity, but rather by its unique interfacial compatibility with electrodes and Zn salts.

MeOH has a relatively high dielectric constant, and when mixed with water at a molar ratio of 1:16, the resulting electrolyte still maintains a high dielectric constant. And MF demonstrated poor electrochemical stability at room temperature, attributable to the intrinsic properties of the solvents. While MF and THF can serve as additives in organic low-temperature electrolytes, MF undergoes hydrolysis in aqueous electrolytes. EA exhibits superior stability compared to MF. The stability of ester groups is influenced by inductive and conjugation effects: (1) The carbonyl carbon in MF is more positively charged due to the weaker electron-withdrawing ability of -H compared to $-CH_3$, rendering it more susceptible to nucleophilic attack. (2) In EA, the methyl group disperses the positive charge of the carbonyl carbon through hyperconjugation, thereby enhancing its stability. (March, J. (1992). Advanced Organic Chemistry (4th ed.). Wiley.)

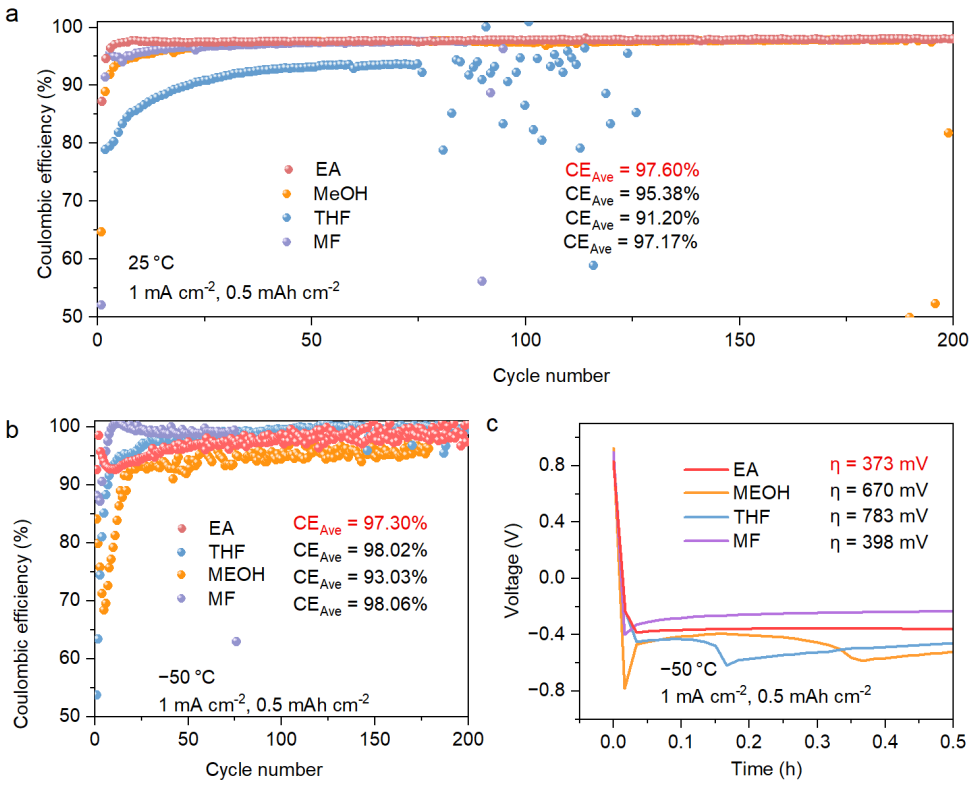

Fig. R18 a, b The CEs of Zn||Cu batteries at a current density of 1 mA cm^{-2} and 0.5 mAh cm^{-2} at 25 °C (a) and −50 °C (b). c, The first discharge curve of Zn||Cu batteries at a current density of 1 mA cm^{-2} and 0.5 mAh cm^{-2}.

Comment 3. The results of Figure S1 show that ZnOTF also enables EA to form a homogeneous solution with H_2O, so why not choose ZnOTF instead of $ZnClO_4$?

Response: Thank you for this important question. Figure S1 indeed shows that Zn(OTf)2 ($Zn(CF_3SO_3)_2$) also yields a single-phase EA:H_2O solution; however, our salt choice is driven by low-temperature transport and interfacial behavior rather than miscibility alone. At identical composition (molar ratio of EA:H_2O =1:16), $Zn(ClO_4)_2$ delivers substantially higher ionic conductivity: 64.47 mS cm^{-1} at 25 °C and 24.92 mS cm^{-1} at −50 °C, versus 41.32 and 10.56 mS cm^{-1} for $Zn(OTf)_2$, respectively (Table R1). This transport advantage translates to cell performance: in Zn||Cu tests (1 mA cm^{-2}, 0.5 mAh cm^{-2}), the $Zn(ClO_4)_2$ EA:H_2O electrolyte exhibits higher Coulombic efficiency, more stable cycling at both temperatures, and a lower nucleation overpotential than the $Zn(CF_3SO_3)_2$ analogue (Fig. R19).

Table R1 Conductivity of $Zn(CF_3SO_3)_2$ EA:H_2O (molar ratio = 1:16) and $Zn(ClO_4)_2$ EA:H_2O (molar ratio = 1:16) measured by the conductivity meter.

Zinc salt	σ (mS cm^{-1})	
	25 °C	−50 °C
$Zn(CF_3SO_3)_2$	41.32	10.56
$Zn(ClO_4)_2$	64.47	24.92

We have added the corresponding content in **Supplementary Note 1**:

"Additionally, $Zn(CF_3SO_3)_2$ enables miscibility of EA and water at a molar ratio of 1:16. Conductivity measurements indicate that $Zn(CF_3SO_3)_2$ in an EA:H_2O mixture (1:16 molar ratio) achieves a conductivity of 41.32 mS cm^{-1} at 25 °C and 10.56 mS cm^{-1} at −50 °C. In contrast, under the same conditions, $Zn(ClO_4)_2$ in EA:H_2O (1:16 molar ratio) exhibits higher conductivities of 64.47 mS cm^{-1} at 25 °C and 24.92 mS cm^{-1} at −50 °C. Thus, the $Zn(ClO_4)_2$-based electrolyte demonstrates superior conductivity at low temperatures, making it a promising candidate for cryogenic applications."

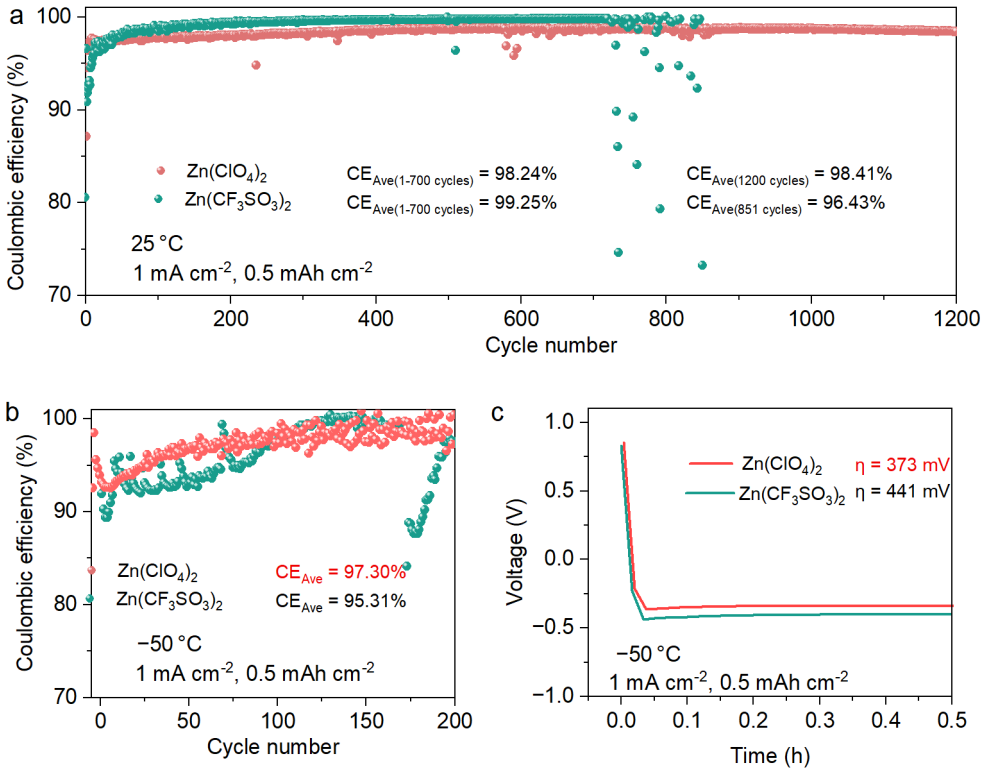

Fig. R19 a, b The CEs of Zn||Cu batteries in $Zn(CF_3SO_3)_2$ EA:H_2O (molar ratio = 1:16) and $Zn(ClO_4)_2$ EA:H_2O (molar ratio = 1:16) at a current density of 1 mA cm^{-2} and 0.5 mAh cm^{-2} at 25 °C (a) and −50 °C (b). c, The first discharge curve of Zn||Cu batteries at a current density of 1 mA cm^{-2} and 0.5 mAh cm^{-2}.

Comment 4. In Line 165, it is stated that weak and medium hydrogen bonding networks evolve to strong hydrogen bonding networks, but the statement is contrary to the cited reference.

Response: Thank you for your comment. As you mentioned, we have corrected our inaccurate descriptions based on the results of Raman and infrared analysis. The Raman spectroscopy with hydrogen-bonded peaks in the 3,100 cm^{-1} to 3,700 cm^{-1} range (Supplementary Fig. 9a). And as shown in Supplementary Fig. 9b-h, the area of peaks representing non-hydrogen-bonded water increases progressively to 60.3% with the rise in EA concentration, indicating the disruption of the hydrogen-bonding network of water. The FTIR result in Fig. 2a, we observed a shift to higher wavenumber in the peaks for cluster water (3335 cm^{-1}) and bulk water (3229 cm^{-1}), along with a shift to lower wavenumber in the peaks for isolated water (3552 cm^{-1}). These results all confirm that the addition of organic cosolvents weakens the hydrogen bond network of water.

We have revised the text on page 7, line 176:

"These results suggest an increased disruption of the hydrogen-bonding network of water and promote the conversion of weak and strong-strength hydrogen bond networks to non-hydrogen bond networks in water, which potentially inhibits the ordered arrangement of water molecules induced by a decrease in temperature."

Comment 5. The results of Fig. 3a, b seems to contradict each other with Fig. 3a showing that MDCE has a greater solvation energy, while the opposite is true for Fig. 3b.

Response: Thank you for the comment. Figure 3a reports the apparent solvation free energy in the bulk electrolyte, inferred from the potentiometric transfer between compositions; this quantity reflects the thermodynamics of the solvated ion, including ion–ion correlations and activity coefficients. In EA-rich MDCE, the lower permittivity promotes contact ion pairs/aggregates around Zn^{2+}, which stabilizes Zn^{2+} in the bulk and renders the apparent solvation free energy more negative.

Figure 3b represents the desolvation energy, indicating the energy barrier for ion desolvation at the interface under an electric field. Based on previous literature reports and our experimental results, it can be concluded that solvents with weak salt dissociation ability can promote ion desolvation. First, the weak ion–solvent interaction reduces the desolvation barrier of the solvated charge-carrier ions and realizes a faster desolvation process. Second, weak ion–solvent interaction means that solvents have limited ability to dissociate salt crystals, which makes anions in the electrolyte more likely to participate in the solvation structure of charge-carrier ions. The resulting strong cation–anion interaction promotes the preferential reduction of anions to form an inorganic-rich SEI film, which accelerates the ion diffusion in the SEI film. (R. Hou, S. Guo, H. Zhou, Atomic Insights into Advances and Issues in Low-Temperature Electrolytes. Adv. Energy Mater. 2023, 13, 2300053)."

Comment 6. Figure S13 only shows that it is easier to remove water molecules in the solvated configuration containing EA formed in the electrolyte after the addition of EA, while the ability of

EA to replace some of the water molecules suggests that it has a stronger bonding force with Zn^{2+}, which may cause a greater obstruction in the removal of EA molecules and ions. Is the statement in the abstract that the modified solvated structure accelerates Zn^{2+} desolvation not appropriate?

Response: Thank you for raising this point. Our previous results demonstrated that the introduction of EA facilitates faster desolvation of water molecules in the Zn^{2+} solvation structure. Furthermore, we performed additional computational analyses to thoroughly assess the stability of the modified solvation structure, offering deeper insights into how EA influences Zn^{2+} desolvation kinetics.

From a dielectric perspective, introducing EA ($\varepsilon \approx 6.4$) markedly diminishes the electrolyte's dielectric shielding capability. This reduction destabilizes the Zn^{2+} solvation shell, driving a transition from a tightly bound, water-dominated configuration to a more loosely coordinated, EA-water mixed structure. Although this electrolyte environment has the single-point binding strength of EA-Zn^{2+}, it overall reduces the rigidity of the solvation shell, making Zn^{2+} more prone to partial desorption. The energy levels (HOMO and LUMO) and molecular orbitals of solvation structures in HDCE and MDCE, compared to the solvation structures without EA, the structure with EA exhibits a narrower HOMO-LUMO energy gap, indicating that the structure containing EA is more susceptible to facilitate the charge transfer reaction under an electric field (J. Am. Chem. Soc. 147, 27802-27811 (2025)), facilitating the Zn^{2+} plating/stripping reactions (Supplementary Fig. 11e).

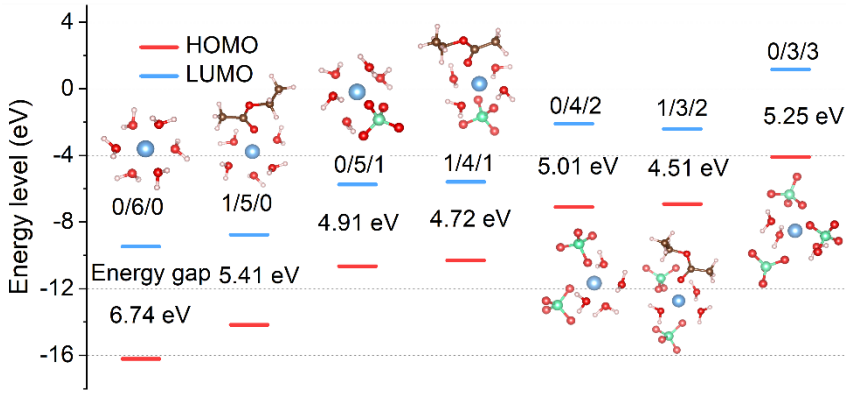

Fig. R20/Supplementary Fig. 11e HOMO/LUMO energy levels and molecular orbitals for solvation structures in HDCE and MDCE; structures are defined by the local fractions of EA/H_2O/ClO_4^-.

Reviewer #4:

The work by Zhu and co-workers presented the performance and characterization of $ZnClO_4$ aqueous electrolytes with or without EA additive. The electrolyte with EA, MDCE, showed superior performance compared to the aqueous counterpart, HDCE, especially at low temperature. The study combined various experimental and simulation techniques and insightful details were provided for the studied systems.

1) The work emphasized "dielectric engineering" in the title. However, the meaning of which is not very clear to me. The study included two electrolytes, one with relative high dielectric and the other one lower. Is the dielectric the decisive reason for the superior performance? If one uses a different additive to prepare an electrolyte with the same dielectric, or even a completely different electrolyte with the same dielectric constant, would the same performance be expected? Or is the performance reported in the work specific for EA at the studied composition?

Response: Thank you for your careful review. The overall dielectric constant (ε) of the electrolyte as a quantitative preliminary screening indicator is a key design criterion for low-temperature aqueous electrolytes.

In our work, "dielectric engineering" means deliberately tuning the bulk permittivity of the solvent matrix by mixing a high-permittivity and a low-permittivity component to place the electrolyte in a medium-permittivity regime. In Zn electrolytes, this regime promotes moderate cation–anion association, lowers effective water activity, and increases the likelihood of anion participation in the primary solvation shell. The combined effect is to support SEI formation at low temperature while retaining adequate ionic transport, resulting in improved battery performance.

While the dielectric is a primary design lever and a quantitative screening metric, it is not sufficient on its own. Different solvents adjusted to the same bulk permittivity can still yield distinct solvation motifs, kosmotropic/chaotropic effects, and reduction pathways; these specific interactions co-determine interfacial kinetics and stability. The trend we emphasize is nevertheless general. For example, Tao et al. used different electrolytes with varying degrees of cation-anion association, including a medium dielectric constant electrolyte 2 M $Zn(BF_4)_2$-AN: H_2O (7:3, v: v)

(ε=46.85), a low dielectric constant electrolyte 2 M $Zn(BF_4)_2$-THF: H_2O (7:3, v: v) (ε=15.28), and a high dielectric constant (ε_{water}=78.46) electrolyte 2 M $Zn(BF_4)_2$-H_2O. They demonstrated that moderate ion association electrolytes using medium-ε solvents like AN can keep high ion transport in the bulk electrolytes and stable anion-derived SEI formation ability on the Zn anode. (*J. Am. Chem. Soc.* 2024, **146**, 46, 31612–31623). This supports targeting a medium-permittivity window rather than any single solvent.

In this work, we selected EA/H_2O (molar ratio 1:16) to construct an electrolyte system with a moderate dielectric constant (ε≈25.25). This design has the following advantages: 1: Greater flexibility in composition: the dielectric environment of the electrolyte can be precisely controlled by adjusting the ratio of high/low dielectric constant solvents. 2: practical screening criterion: providing a quantifiable preliminary screening criterion for the design of low-temperature-resistant aqueous electrolytes. However, the permittivity is a screening variable, not a sole determinant (solvent identity still matters).

We have provided corresponding supplementary descriptions in the main text (page 3, line 69):

"we proposed a dielectric matching strategy, placing the aqueous electrolyte in a medium-permittivity window by mixing a high-ε and a low-ε component. Wherein high-ε solvents promote the dissociation of zinc salts and low-ε solvents optimize interface stability and ion transport kinetics at low temperatures."

2) Other specific comments:

a) Line 130, "pure electrolyte" likely means "pure aqueous electrolyte", but it could also mean "pure EA electrolyte". Please clarify.

Response: Thank you for pointing out the problem. Thank you for catching these ambiguities. We now write "The electrolyte without EA" instead of "pure electrolyte" in main text on page 5, line 135:

"The electrolyte without EA has a crystallization temperature (T_c) of −38.5 °C, and adding EA at a 1:20 ratio reduced the crystallization temperature to −51.3 °C."

b) Line 138: "nEA:nH_2O" should be "EA:H_2O".

Response: Thank you for catching these ambiguities. We have corrected "nEA:nH_2O" to EA:H_2O in the main text on page 5, line 142:

"Among the tested EA:H_2O ratios, 1:16 delivered the highest ionic conductivity at −50 °C (24.92 mS cm^{-1})"

c) Starting from Line 155, the authors discussed the FTIR results. The authors mentioned "red shift" and "blue shift", but it is hard to see from the context the shifts are relative to what. On lines 162-163, the terms "left shift" and "right shift" were used whereas Figures 2a and 2b show FTIR in opposite frequency orders, which make it hard to follow. These terms are not professional either. Opposite x-axis is also seen in Figure 6 in SI. Please make it consistent throughout the paper.

Response: Thank you for flagging the ambiguity and axis inconsistencies. We standardized all FTIR plots to the same axis orientation—decreasing wavenumber from high to low—across the main text and SI (updated Figs. 2a, b and Supplementary Figs. 8), and we revised captions to state the reference and axis direction. To quantify changes, spectra were baseline-corrected and deconvolved. The C–O–C mode shifts from 1046 to 1040 cm^{-1} and the O–Cl–O mode from 1079 to 1073 cm^{-1} with EA addition. Peak assignments used in the analysis are: SSIP (non-coordinated ClO_4^-, 1076 cm^{-1}), CIP (Zn–$(ClO_4^-)_{n\geq1}$, 1047 cm^{-1}), free anion (1114 cm^{-1}), and free EA (1037 cm^{-1}). Area evolution shows a decrease of SSIP and free-anion contributions and a corresponding increase of CIP, consistent with enhanced anion participation in the primary solvation shell. Spectra were baseline-corrected and fitted with Voigt profiles using shared-width constraints; peak positions, FWHM, and integrated areas were extracted. These revisions remove ambiguity and make the comparison reproducible.

We have added the corresponding content in the manuscript on page 6, line 162:

"To comprehensively understand the molecular mechanisms of different segments in MDCE, the coordination of Zn^{2+} with ClO_4^- anions were investigated by FTIR spectroscopy (Supplementary Fig. 8c, d). The results show peaks assigned to separated ion pairs (SSIPs, noncoordinated ClO_4^-, 1076 cm^{-1}), contact ion pairs (CIPs, Zn-$(ClO_4^-)_{n\geqslant1}$, 1047 cm^{-1}), indicating strong adsorption for ClO_4^-, free anion (1114 cm^{-1}) and free EA (1037 cm^{-1}). The results indicate that upon the

introduction of EA, the content of SSIP and free anions in the electrolyte decreases, while the concentration of CIP increases. Additionally, a fraction of EA exists as free solvent."

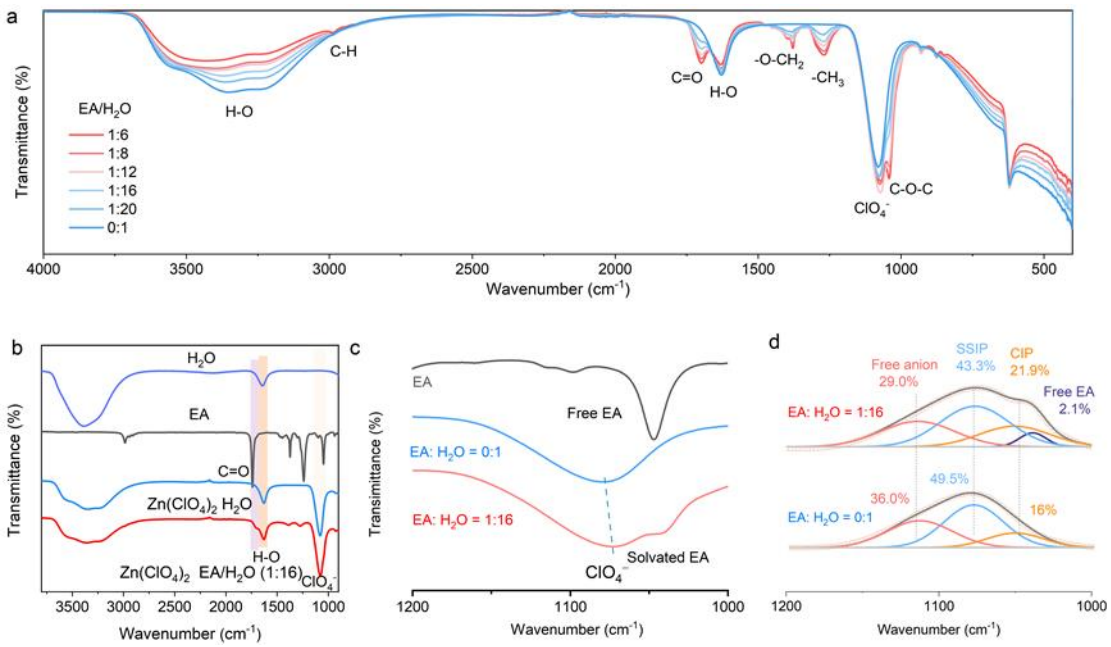

Fig. R22/Supplementary Fig. 8 a, FTIR spectra of 2 M $Zn(ClO_4)_2$ H_2O/EA electrolytes with different EA:H_2O ratios from 0:1 to 1:6 at 4,000–400 cm^{-1}. b, c FTIR spectra of H_2O, EA, 2 M $Zn(ClO_4)_2$ H_2O and 2 M $Zn(ClO_4)_2$ EA:H_2O (EA:H_2O = 1:16) electrolytes at 3,800–800 cm^{-1} (b) and 1,200–1,000 cm^{-1} (c). d, Deconvolution result of FTIR spectra for 2 M $Zn(ClO_4)_2$ H_2O and 2 M $Zn(ClO_4)_2$ EA:H_2O (EA:H_2O = 1:16) electrolytes at and 1,200–1,000 cm^{-1}.

d) Line 185 mentioned average number of HB but it is not clear average over what? Are the numbers per water molecule or per acceptor site or any other definition?

Response: Thank you for pointing out the problem. The average number of HB is per acceptor site (water or EA), including water and EA. The calculation formula is as follows:

$$\text{Average HBs} = \frac{\text{Total number of HBs}}{\text{Total number of acceptor sites for all molecules}}$$

We have added the corresponding calculation methods in the manuscript on page 24, line 633:

"The calculation formula for the average value of hydrogen bonds is as follows:

$$\text{Average HBs} = \frac{\text{Total number of HBs}}{\text{Total number of acceptor sites for all molecules}} \quad (4)$$

”

e) For the FTIR results shown in Figure 2, what is the temperature? Does FTIR show the same temperature dependent trend as the simulation? Temperature is not provided for most of the results reported in the manuscript.

Response: Thank you for highlighting this. The FTIR spectra in Figure 2 were collected at 25 °C; we now state the temperature explicitly in the figure caption and in Methods. We also standardized temperature reporting across the manuscript (electrochemistry, spectroscopy, and conductivity), and corrected axis labels where needed for consistency:

“*In situ* electrochemical FTIR was performed on a Vertex 70 spectrometer (Bruker) coupled to a CHI760E workstation and equipped with a liquid-nitrogen-cooled broadband MCT detector at room temperature. (Page 22, line 579);

Confocal imaging employed a Leica TCS SP5II system with 458 nm excitation and 490-550 nm detection range using a 20× dry objective at room temperature. (Page 22, line 592);

A confocal Raman microscope (Renishaw, inVia-Reflex) equipped with a green diode laser (λ = 532 nm) was used for the Raman analysis at room temperature. (Page 23, line 597);

The conductivity of the electrolyte at 25°C, 0°C, −20°C, −40°C, and −50°C was measured using the Mettler Toledo Conductivity Meter (FE38-Standard). (Page 22, line 607)”

f) The sentences on lines 229-233 are hard to follow. In the beginning it mentioned “immobilization of the ClO_4^- anion”, what does “immobilization” mean here? Then it talks about solvents: “solvents with stronger binding properties tend to produce more negative solvation energies”. In the next sentence, it goes back to ion: “corresponding to a greater number of ion pairs.” Then the final part, what does “reduced ion dissociation” mean? Is this about structure or kinetics?

Response: The phrase "immobilization of the ClO_4^- anion" indicates that ClO_4^- serves as the fixed anionic component in both HDCE and MDCE systems. Different anion salts may influence the test results, all electrolytes used in this study are zinc salts containing ClO_4^- anions. This eliminates the need for extensive discussion of alternative anion systems, thereby avoiding potential reader confusion or misinterpretation regarding other salt types, so we removed this sentence from the main text.

Since solvation energy measurements can be influenced by both the solvent and the salt composition, we specifically employed ClO_4^- as the sole anion throughout this study to isolate and compare the effects of different solvents on solvation energy. "Reduced ion dissociation" refers to the ability of a solvent to dissociate cation-anion pairs. Solvents with low dielectric constants have poor ion dissociation capabilities, adding a low dielectric constant solvent to a high dielectric constant solvent can reduce the degree of ion dissociation in the high dielectric constant electrolyte, thereby increasing the number of ion pairs in the high dielectric constant electrolyte. To enhance clarity and avoid redundancy, we have revised the manuscript language in main text on page 9, line 245:

"Because stronger binding yields more negative solvation free energies, the more negative ΔG_{solv} measured for MDCE (Fig. 3a; Supplementary Table 6) indicates tighter Zn^{2+} binding and, correspondingly, a higher fraction of ion pairs in the liquid[37]."

[37] Wang, H., Kim, S. C., Rojas, T., Zhu, Y., Li, Y., Ma, L., Xu, K., Ngo, A. T. & Cui, Y. Correlating Li-ion solvation structures and electrode potential temperature coefficients. *J. Am. Chem. Soc.* **143**, 2264-2271 (2021).

g) Lines 240-241: E_a were reported for HDCE and MDCE, and commented that "the latter (MDCE) being notably lower than …" The E_a of HDCE and MDCE are only 1.2 kJ/mol different from each other, which is lower than kT. These E_a are similar to me.

Response: Thank you for the insightful comment regarding the apparent similarity in activation energies (E_a) between HDCE and MDCE. First, although the desolvation energy difference

between HDCE and MDCE is relatively small, based on the Arrhenius equation ($k = Ae^{-\frac{E_a}{RT}}$), it can be inferred that the zinc ion desolvation rate in MDCE is 1.623 times that of HDCE:

$$\frac{k_{MDCE}}{k_{HDCE}} = e^{\frac{-(E_{aMDCE}-E_{aHDCE})}{RT}} = 1.623$$

A relatively small difference in desolvation energy can also significantly impact the reaction rate. Moreover, the resulting E_a values were 22.1 kJ mol^{-1} for HDCE and 20.9 kJ mol^{-1} for MDCE, with the latter being notably lower than values reported for most comparable electrolyte systems.

Our use of "notably lower" referred to comparison with many reported electrolytes rather than to HDCE specifically. For context, the table below compiles representative values (Table R2).

Table R2 Compared with the desolvation energy reported in previous literature.

Electrolyte	E_a (kJ mol^{-1})	Ref
2 M $Zn(OTf)_2$ TMP/H_2O volume ratios of 2:3	54.8	Nat Commun 14, 5443 (2023)
0.5 M $Zn(SO_4)_2 \cdot 7H_2O$ butanone/H_2O volume ratios of 1:7	30.6	Nat Commun 15, 302 (2024)
2 M $Zn(OTf)_2$ sulfolane/H_2O weight ratios of 0:1	41.65	Nat Commun 14, 3067 (2023)
2 M $Zn(OTf)_2$ sulfolane/H_2O weight ratios of 3:7	65.15	Nat Commun 14, 3067 (2023)
$Zn(Ac)_2$/Fad molar ratios of 1:9	22.53	Angew. Chem. Int. Ed. 2024, 63, e202406906.
2 M $Zn(ClO_4)_2$ EA/H_2O molar ratios of 0:1 (HDCE)	22.1	This work
2 M $Zn(ClO_4)_2$ EA/H_2O molar ratios of 1:16 (MDCE)	20.9	This work

h) Line 578 says the OPLS-AA force field was used in the study. Does OPLS-AA include parameters for Zn^{2+} ion? If not, please specify what model was used for Zn^{2+}.

Response: Thank you for pointing this out. The built-in OPLS-AA force field does not include parameters for Zn^{2+} ions. In our study, we employed a Zn^{2+} model based on parameters reported in a previous publication (*J. Chem. Theory Comput. 2020, 16, 4429−4442*), which we further optimized for aqueous zinc battery simulations. The employed Zn^{2+} model has been validated in several previous studies (e.g., *Adv. Mater. 2025, 2502649*; *Adv. Funct. Mater. 2022, 32, 2109322*), and has demonstrated good accuracy in reproducing the solvation structure and transport behavior of Zn^{2+} in aqueous electrolytes.

The fit results of EXAFS also confirmed the validity of the OPLS-AA force field. The $Zn\text{-}O_{(H2O)}$ $Zn\text{-}O_{(ClO4)}$ and $Zn\text{-}O_{(EA)}$ bond length in $Zn(H_2O)_5(ClO_4)^+$ and $Zn(H_2O)_4EA(ClO_4)^+$ acquired by MD simulation, EXAFS fitting, and DFT calculation are consistent within the error of 5% and summarized in Table R3.

Table R3. The bond length of Zn–O in HDCE and MDCE by MD simulation, EXAFS fitting, and DFT calculation.

Method	Path	MD R (Å)	DFT R (Å)	RDF R (Å)
HDCE (path in $Zn(H_2O)_5(ClO_4)^+$)	Zn-O (H_2O)	2.13	2.14	2.04
	Zn-O (ClO_4)	2.09	2.09	2.01
MDCE(path in $Zn(H_2O)_4EA(ClO_4)^+$)	Zn-O (H_2O)	2.13	2.16	2.04
	Zn-O (ClO_4)	2.09	2.14	2.01
	Zn-O (EA)	2.15	2.07	2.06

i) For the simulation study, validation of the force field needs to be provided.

Response: Thank you for raising this point. We have noted the previously reported examples: OPLS-AA combined with the Zn^{2+} model has been successfully applied to aqueous Zn electrolytes, reproducing solvation structure and transport trends (e.g., *Proc. Natl. Acad. Sci.* **120**, e2221980120 (2023), *Nat. Commun.* **16**, 3820 (2025), *Nat. Commun.* **16**, 5740 (2025), *Nat. Commun.* **15**, 6471 (2024), *Nat. Commun.* **16**, 1273 (2025), *Nano-Micro Lett.* **18**, 3 (2025), *J. Am. Chem. Soc.* **144**,

7160-7170 (2022), *Energy Environ. Sci.* **13**, 3527-3535 (2020), *Adv. Mater.*, 2502649. https://doi.org/10.1002/adma.202502649, *ACS Energy Lett.* **8**, 608-618 (2023)). These works collectively support the validity and applicability of the OPLS-AA force field for modeling the structural and transport properties of aqueous zinc battery systems.

Overall, the work presented a systematic study of an electrolyte system and insightful results were reported. An emphasis on dielectric engineering was made. However, it is not clear what the authors mean by "dielectric engineering". On the other hand, the effect of dielectric constant has been discussed in the literature. Works on low temperature electrolyte are available in the literature too. Therefore, I do not think the work carry enough novelty to be published in Nature Communication. I would suggest the authors address above comments and resubmit it to a different journal.

Response: Thank you for the suggestions. We agree that the manuscript needed a clearer definition of "dielectric engineering" and a sharper articulation of what is new. We will respond to the reviewers' questions as follows:

First, we clearly define the specific meaning of "dielectric engineering" in the context of this study. This study proposes a dielectric matching strategy based on the physical property of the solvent's dielectric constant (ε), whereby high-ε solvents facilitate zinc salt dissociation and low-ε solvents optimize interface film formation.

Second, the reviewers noted that previous studies have discussed dielectric constants and low-temperature electrolytes. Our work fundamentally differs from these previously reported studies for the following reasons:

1) Mechanism difference.

This study presents differences in mechanisms compared to previous research. Chen et al. aim to facilitate coordination of the low-ε solvents with Li^+ to occupy its coordination sites, thus converting the solvent-separated ion pairs (SSIPs) from high-ε solvent-dominated to low-ε-dominated (*Nat. Commun.* 14, (2023): 8326). Yang et al. (*Nat. Sustain.* 6, 325–335 (2023)) and Wang et al. (*Nat Commun.* 14, 2023: 5443) other researchers have predominantly focused on how the regulation of solvation structures by co-solvents enhances low-temperature performance,

without in-depth investigation into the evolution of interfacial solvation structures under an electric field and their role in promoting SEI formation.

We proposed a dielectric matching strategy, wherein high-ε solvents promote the dissociation of zinc salts, while low-ε solvents optimize interface stability and ion transport kinetics at low temperatures. And we focus on exploring how the dielectric properties of co-solvents affect their solvation structure, and clarify their relationship with low-temperature ion transport dynamics and cycling stability.

2) Deeper consideration of the challenges posed by low-temperature conditions.

Some studies have reported regulating the solvation structure to lower the crystallization temperature of electrolytes, while suppressing HER (hydrogen evolution reaction) and Zn dendrite growth. However, the following issues remain to be addressed: 1. Although the freezing point of electrolytes can be effectively reduced, this is often achieved at the expense of ion transport kinetics. Minimizing the loss of ionic conductivity under ultra-low temperature conditions while maintaining the stability of the solvation structure is key to achieving efficient zinc ion transport. To address this, we selected chaotropic ClO_4^- anions, which exhibit strong hydrogen bond disruption capabilities, along with low-viscosity ethyl acetate, to minimize the ionic transport impedance at low temperatures. 2. The cycle life of existing low-temperature zinc metal anodes is generally limited to a few hundred hours, which is insufficient for practical applications. To overcome the limitations of cycle stability, we investigated how low dielectric constant influences the regulation of interfacial solvation structure, promoting SEI formation and the potential mechanism for reversible deposition/dissolution at low temperatures. Our zinc metal anode symmetrical cell provides an ultra-long time of 7,200 hours of stable cycling at 25 °C, and 4,000 hours at the ultra-low temperature of −50 °C with an ultra-thin zinc foil of 30 μm.

3) Deeper investigation into interfacial electrochemical reactions.

Most work has focused on how the regulation of solvation structures by co-solvents enhances low-temperature performance, lacking in-depth investigation into the evolution of interfacial solvation structures under an electric field and their role in promoting SEI formation. We addressed this issue by employing advanced *in-situ* characterization techniques. For the first time, *in situ* two-dimensional pH characterization was conducted using confocal laser scanning microscopy (CLSM) to monitor the HER of the electrolyte. Operando infrared elucidates interfacial dynamics

and decomposition mechanisms under an electric field, providing insights into solid/liquid interfaces and solvation dynamics crucial for cryogenic aqueous batteries.

We emphasize generality over solvent specificity; EA is a useful example of the medium-ε strategy. The revised text now presents dielectric engineering as a practical screening criterion, including permittivity range and solvation/interfacial checks, clarifies how our mechanism goes beyond a single cosolvent, and places the results within the context of existing literature. We hope these clarifications and additions address the reviewer's concerns about definition and novelty.

Response to the reviewers' comments

We sincerely appreciate the reviewer's endorsement of our work, and their insightful and constructive input. The manuscript has now been carefully revised, and the revisions are highlighted by yellow color. Our point-to-point responses to the comments are given in the following.

Reviewer #1:

Comment: This manuscript has been revised as the comments, so it is suitable for publication without change.
Response: Thank you for your endorsement of our work.

Reviewer #2:

Comment: The authors provided a complete response to my questions. I suggest the consideration of this work.
Response: Thank you for your endorsement of our work.

Reviewer #3:

Comment: All my questions have been well addressed. It can be accepted in this journal.
Response: Thank you for your endorsement of our work.

Reviewer #4:

Comment: The authors addressed most of my comments. But critical details of the MD simulations are still missing. The authors said an optimized Zn2+ model was used in the study. The parameters, reference and/or other optimization details should be provided so that readers can reproduce the work.

Proper validation of the used force fields parameters for the studied systems are also needed. General force fields like OPLS can work on one system but fail badly on another. The choice of water model and other simulation protocols can change the results too. In spite of the references provided, direct comparison with experimental measurement on the same systems should be provided.

Response: We thank the reviewer for the insightful and thoughtful comment.

We agree with the reviewer that the OPLS-AA force field may present limitations in accurately describing Zn^{2+} systems. To comprehensively address this concern, we revalidated our previous MD simulations using the AMBER force field. In the new AMBER-based simulations, we employed the Zn^{2+} parameters developed by Merz and co-workers (Lennard–Jones 12–6, IOD parameter set, compatible with the OPC water model) [*J. Chem. Theory Comput. 2020, 16, 4429−4442*]. The results indicate that the solvation structure, dielectric constant, and hydrogen-bonding characteristics obtained from the AMBER force field are consistent with those derived from OPLS-AA, with

only minor deviations that do not alter our main conclusions. **To fully address the reviewer's concerns, all MD simulation results in the manuscript have been replaced with those obtained from the AMBER force field**, and the corresponding sections have been revised accordingly. The specific changes are detailed below.

We have added the relevant MD simulation details in Calculation part from the main text (page 23, line 614) as:

"Molecular dynamics (MD) calculations: MD simulations were carried out using GROMACS[57] 2024.4. The AMBER force field[58], OPC water model[59] and restrained electrostatic potential (RESP) charge (obtained with Multiwfn[60]) were employed with previously reported Zn^{2+} parameter of Lennard-Jones 12-6 model (IOD set)[61].

58 Wang, J., Cieplak, P. & Kollman, P. A. How well does a restrained electrostatic potential (resp) model perform in calculating conformational energies of organic and biological molecules? *J. Comput. Chem.* **21**, 1049-1074 (2000).

59 Izadi, S., Anandakrishnan, R. & Onufriev, A. V. Building water models: A different approach. *J. Phys. Chem. Lett.* **5**, 3863-3871 (2014).

60 Lu, T. & Chen, F. Multiwfn: A multifunctional wavefunction analyzer. *J. Comput. Chem* **33**, 580-592 (2012).

61 Li, Z., Song, L. F., Li, P. & Merz, K. M., Jr. Systematic parametrization of divalent metal ions for the opc3, opc, tip3p-fb, and tip4p-fb water models. *J. Chem. Theory Comput.* **16**, 4429-4442 (2020)."

To fully address the reviewer's concerns regarding the use of OPLS-AA for calculating Zn^{2+}, we have replaced all MD calculations with the AMBER force field-based simulations as below:

1. Solvation structure analysis

Under identical computational conditions, the radial distribution functions (RDF) and coordination number values generated by both methods exhibited similar results. The MD simulations presented in Figures R1 and R2 employed AMBER force fields, while Figure R3 utilized the OPLS-AA force field. We have updated the corresponding results accordingly on page 8, line 211:

"For MDCE, as the temperature decreased from 25 °C to −50 °C, the average CN of Zn^{2+} with oxygen in EA and ClO_4^- increased slightly, from 0.19 to 0.21 and from 1.35 to 2.12, respectively (Fig. 2f and Supplementary Fig. 11d)."

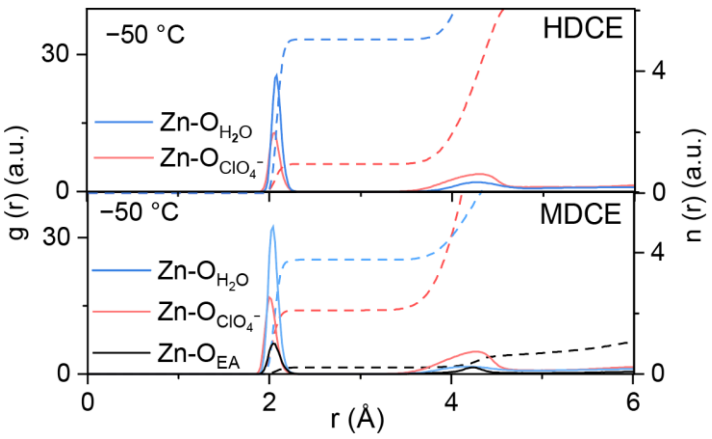

Fig. R1/Fig. 2f. Distributions of Zn^{2+} solvation species and RDFs/CNs in MDCE and HDCE at −50°C.

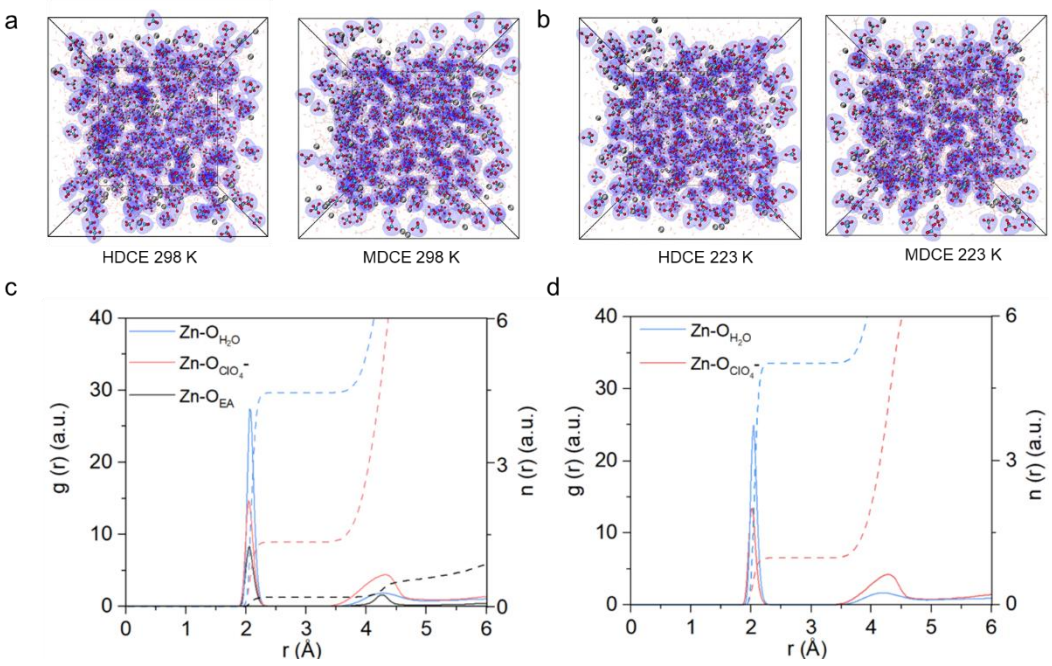

Fig. R2/Supplementary Fig. 11. (a,b) Snapshots of representative Zn^{2+} solvation motifs in HDCE and MDCE at 25 °C (a) and −50 °C (b); anion distributions are highlighted. (c,d) Distributions of Zn^{2+} solvation species and RDFs/CNs in MDCE (c) and HDCE (d) at 25 °C.

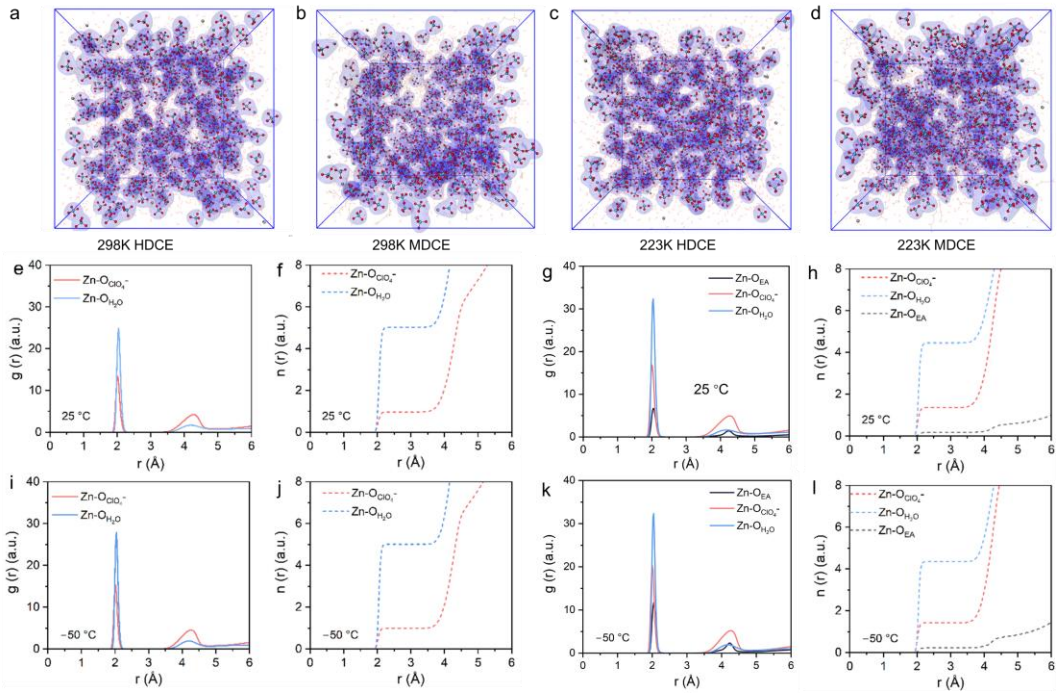

Fig. R3 (a-d) Snapshots of representative Zn^{2+} solvation motifs in HDCE (a, c) and MDCE (b, d) at 25 °C and −50 °C; anion distributions are highlighted. (e-h) Distributions of Zn^{2+} solvation species and RDFs in HDCE (e, f) and MDCE (g, h) at 25 °C. (i-l) Distributions of Zn^{2+} solvation species and RDFs in HDCE (i, j) and MDCE (k, l) at −50 °C.

We performed a comprehensive statistical analysis of the solvation structures. The statistical results reveal similar distributions of solvation structures across different force field implementations. Figure R4 presents results obtained using AMBER force field, while Figure R5 displays results obtained using OPLS-AA force fields.

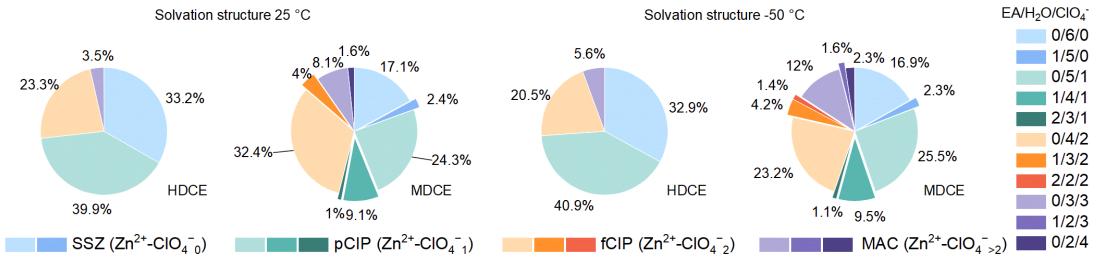

Fig. R4/Fig. 2g Distribution of primary solvation structures obtained from MD simulations.

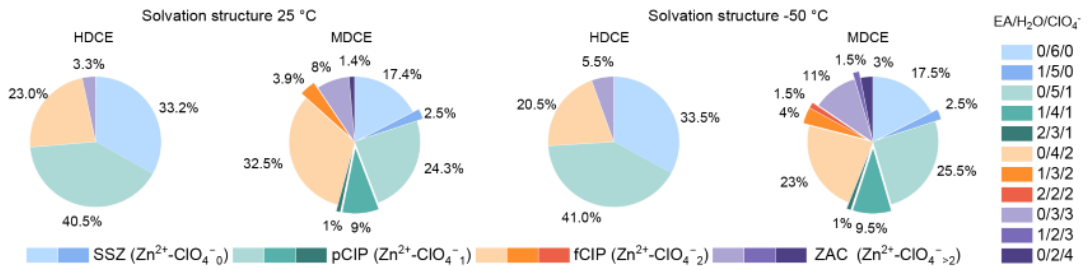

Fig. R5 Distribution of primary solvation structures obtained from MD simulations.

2. Statistics of hydrogen bonds

We conducted a statistical analysis of the solvation structures, which revealed similar average numbers of hydrogen bonds across different force fields. The results presented in Figures R6 and R7 were obtained using AMBER force fields, while Figures R8 and R9 show results from OPLS-AA force fields. The corresponding statistical data have been updated accordingly on page 8, line 200:

"At 25 °C, the nHBs for HDCE and MDCE were calculated to be 2.32 and 2.03, respectively (Supplementary Fig. 12). Upon cooling to −50 °C, HDCE exhibited a substantial increase in hydrogen bonding, with nHBs rising to 2.69, as visualized by the color change in Fig. 2e. In contrast, MDCE showed a more moderate increase, with nHBs reaching only 2.28 (Fig. 2d)."

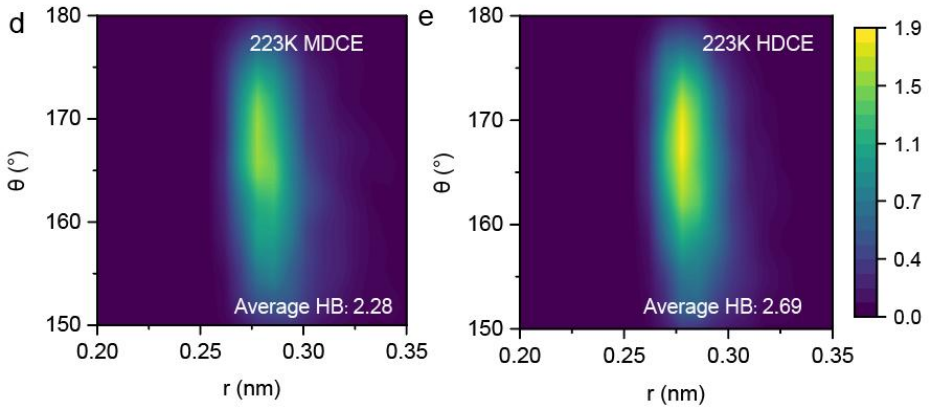

Fig. R6/Fig. 2d, e Radial angular distribution functions, g(r, θ), for MDCE and HDCE at 223 K.

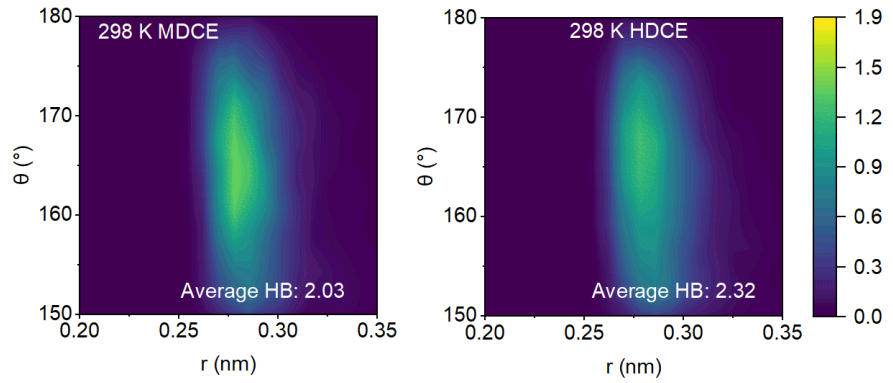

Fig. R7/Supplementary Fig. 12 Radial angular distribution functions, g(r, θ), for MDCE and HDCE at 298 K.

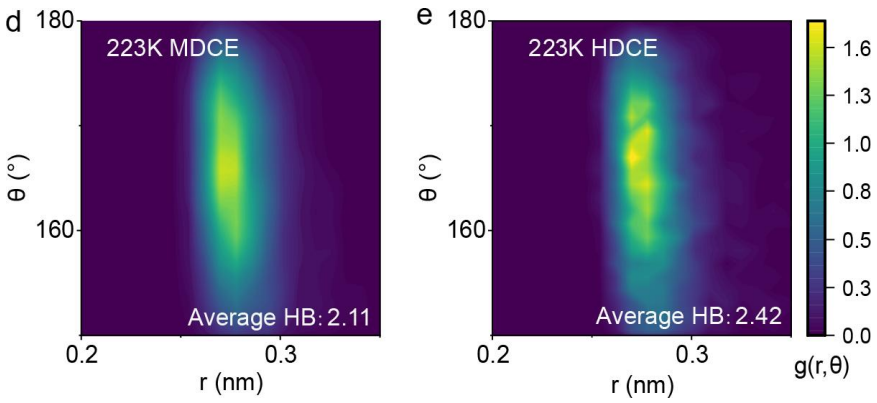

Fig. R8 Radial angular distribution functions, g(r, θ), for MDCE (d) and HDCE (e) at 223 K.

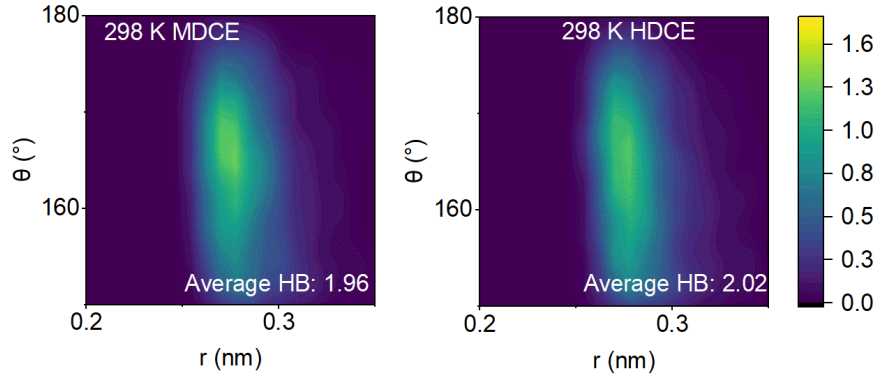

Fig. R9 Radial angular distribution functions, g(r, θ), for MDCE and HDCE at 298 K.

3. Calculation of dielectric constant

We recalculated the dielectric constant. The results presented in Figures R10 were obtained using AMBER force fields, while Figures R11 show results from OPLS-AA force fields. The corresponding statistical data have been updated accordingly on page 5, line 122:

"The dielectric constant of the $Zn(ClO_4)_2/H_2O$ electrolyte is 42.48, categorizing it as a high-dielectric-constant electrolyte (HDCE). In contrast, the $Zn(ClO4)_2$/EA electrolyte exhibits a much lower dielectric constant of 5.47. When $Zn(ClO_4)_2$ is dissolved in a water-EA mixture, the resulting electrolyte has an intermediate dielectric constant of 24.13 (Fig. 1e), and is thus designated as a medium-dielectric-constant electrolyte (MDCE)."

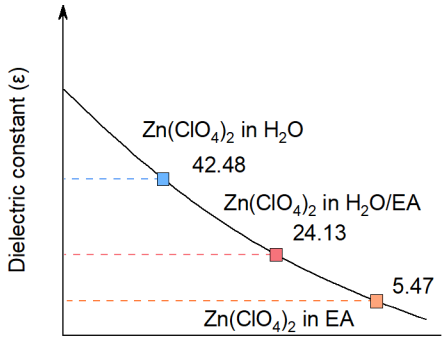

Fig. R10/Fig. 1e ε values of 2 M $Zn(ClO_4)_2$ in H_2O, 2 M $Zn(ClO_4)_2$ in H_2O/EA (EA/H_2O = 1:16, molar ratio) and 2 M $Zn(ClO_4)_2$ in EA electrolytes.

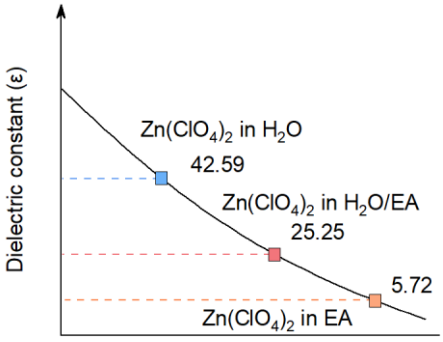

Fig. R11 ε values of 2 M $Zn(ClO_4)_2$ in H_2O, 2 M $Zn(ClO_4)_2$ in H_2O/EA (EA/H_2O = 1:16, molar ratio) and 2 M $Zn(ClO_4)_2$ in EA electrolytes.

We sincerely thank the reviewers once again. Their insightful comments have greatly improved the quality and clarity of our manuscript. We hope that the revisions made in response will fully address the reviewer's concerns.

Response to the reviewers' comments

We sincerely appreciate the reviewer's endorsement of our work, and their insightful and constructive input. The manuscript has now been carefully revised, and the revisions are highlighted by yellow color. Our point-to-point responses to the comments are given in the following.

Reviewer #4:

Comment: The authors provided more simulation details including information about the force field parameters in the revised manuscript. Considering the fact that simulation is only part of this work, I would support the publication of the work if the authors can provide input files for the simulation in the SI, including enough information about simulation details and all the force field parameters that others can reproduce the work.

Meanwhile, I want to make it clear to the authors that consistent results using two sets of force fields do not necessarily validate the simulation results. As I commented previously, a direct comparison with experimental measurements on the same system under the same condition is needed for this purpose.

Response: We sincerely thank the reviewer for the supportive comments. Following this suggestion, we have now included a set of simulation details and the force field parameters in the Supporting Information (SI) as following:

More details are provided for the MD simulations: The parameters of Zn^{2+} were obtained from previously reported research[7], ($R_{min,M}/2$ = 1.373Å, ε_M = 0.01179373 kcal mol^{-1}). The parameters of ClO_4^- and EA were generated with Sobtop[8]. The simulations were conducted using AMBER force field with the OPC water model. The production MD simulation was performed for 20 ns with a time step of 1 fs using the leap-frog integrator. Bond constraints were handled using the LINCS algorithm with an order of 4 and one iteration. A Verlet cutoff scheme was employed for neighbor searching with a frequency of 10 steps. Both the short-range electrostatic and van der Waals cutoffs were set to 1.0 nm. Long-range electrostatic interactions were treated using the Particle Mesh Ewald (PME) method with a fourth-order interpolation and a Fourier grid spacing of 0.16 nm. The temperature was maintained at 298 K or 223K using the Nosé-Hoover thermostat with a time constant of 0.5 ps applied to the system. The pressure was controlled at 1.0 bar using the Parrinello-Rahman barostat with isotropic coupling, a time constant of 2.0 ps, and a compressibility of 4.5×10^{-5} bar^{-1}. Periodic boundary conditions were applied in all three directions.

7 Li, Z., Song, L. F., Li, P. & Merz, K. M., Jr. Systematic parametrization of divalent metal ions for the OPC3, OPC, TIP3P-FB, and TIP4P-FB water models. J. Chem. Theory Comput. 16, 4429-4442 (2020).

8 Lu, T. Sobtop, version 1.0(dev5), http://sobereva.com/soft/Sobtop (2025).

We sincerely appreciate the reviewer's insightful comment and fully concur that experimental comparison is the gold standard for validation. We will be more mindful of this in our future work. Thank you.